

Association of an A-Kinase-anchoring Protein Signaling Scaffold with Cadherin Adhesion Molecules in Neurons and Epithelial Cells

Jessica A. Gorski,* Lisa L. Gomez,* John D. Scott,[†] and Mark L. Dell'Acqua*[‡]

*Department of Pharmacology and [†]Program in Neuroscience, University of Colorado at Denver and Health Sciences Center, Aurora, CO 80045; and [‡]Howard Hughes Medical Institute, Vollum Institute, Oregon Health Sciences University, Portland, OR 97201

Submitted February 16, 2005; Revised May 17, 2005; Accepted May 19, 2005
Monitoring Editor: Asma Nusrat

A-kinase-anchoring protein (AKAP) 79/150 organizes a scaffold of cAMP-dependent protein kinase (PKA), protein kinase C (PKC), and protein phosphatase 2B/calcineurin that regulates phosphorylation pathways underlying neuronal long-term potentiation and long-term depression (LTD) synaptic plasticity. AKAP79/150 postsynaptic targeting requires three N-terminal basic domains that bind F-actin and acidic phospholipids. Here, we report a novel interaction of these domains with cadherin adhesion molecules that are linked to actin through β -catenin (β -cat) at neuronal synapses and epithelial adherens junctions. Mapping the AKAP binding site in cadherins identified overlap with β -cat binding; however, no competition between AKAP and β -cat binding to cadherins was detected in vitro. Accordingly, AKAP79/150 exhibited polarized localization with β -cat and cadherins in epithelial cell lateral membranes, and β -cat was present in AKAP-cadherin complexes isolated from epithelial cells, cultured neurons, and rat brain synaptic membranes. Inhibition of epithelial cell cadherin adhesion and actin polymerization redistributed intact AKAP-cadherin complexes from lateral membranes to intracellular compartments. In contrast, stimulation of neuronal pathways implicated in LTD that depolymerize postsynaptic F-actin disrupted AKAP-cadherin interactions and resulted in loss of the AKAP, but not cadherins, from synapses. This neuronal regulation of AKAP79/150 targeting to cadherins may be important in functional and structural synaptic modifications underlying plasticity.

INTRODUCTION

Elucidating how signaling pathways are organized within cells is key to understanding unique functions of different specialized cell types. In many cases, common transduction pathways are adapted to cell-specific functions through combinatorial assemblies of signaling proteins coordinated by anchoring and scaffolding proteins (Smith and Scott, 2002). In excitatory neurons, postsynaptic N-methyl-D-aspartate and α -amino-3-hydroxy-5-methylisoxazole-4-propionic acid glutamate receptors (NMDAR and AMPAR) are localized to a structure called the postsynaptic density (PSD), where they are linked to the actin cytoskeleton, scaffold

proteins, and signaling proteins. In long-term potentiation (LTP) and long-term depression (LTD) synaptic plasticity underlying learning and memory, NMDARs control synaptic strength through kinases and phosphatases that regulate AMPAR channel properties and PSD localization. Specifically, LTP increases, whereas LTD decreases, AMPAR activity and PSD localization (Malenka and Bear, 2004).

AKAP79/150 (human 79/rat 150), a cAMP-dependent protein kinase (PKA), protein kinase C (PKC), and protein phosphatase 2B/calcineurin (CaN) anchoring protein, is an important postsynaptic scaffold regulating AMPAR phosphorylation in these pathways (Bauman *et al.*, 2004). AKAP79/150 is linked to NMDARs and AMPARs in the PSD through binding the postsynaptic density-95, discs large, zona occludens-1 (PDZ) domain membrane-associated guanylate kinase (MAGUK) scaffold proteins postsynaptic density-95 (PSD-95) and synapse-associated protein-97 (SAP97) (Colledge *et al.*, 2000). PKA phosphorylation increases AMPAR channel open probability and is necessary for synaptic stabilization of AMPARs recruited by LTP (Banke *et al.*, 2000; Esteban *et al.*, 2003; Lee *et al.*, 2003). Conversely, LTD involves CaN and protein phosphatase 1 (PP1) dephosphorylation and CaN-dependent endocytic AMPAR removal (Lee *et al.*, 2000; Carroll *et al.*, 2001). Importantly, disruption of AKAP-PKA anchoring leads to CaN-dependent, LTD-like down-regulation of AMPAR currents, thus implicating AKAP79/150 in AMPAR regulation (Tavalin *et al.*, 2002).

To accommodate AMPAR insertion or removal, the physical structure of synapses is also dynamic. At mature syn-

This article was published online ahead of print in *MBC in Press* (<http://www.molbiolcell.org/cgi/doi/10.1091/mbc.E05-02-0134>) on June 1, 2005.

Address correspondence to: Mark L. Dell'Acqua (mark.dellacqua@uchsc.edu).

Abbreviations used: AKAP, A-kinase-anchoring protein; AMPAR, α -amino-3-hydroxy-5-methylisoxazole-4-propionic acid receptor; α -cat, α -catenin; β -cat, β -catenin; CaN, protein phosphatase 2B/calcineurin; Ecad, E-cadherin; FRET, fluorescence resonance energy transfer; LTD, long-term depression; LTP, long-term potentiation; MAGUK, membrane-associated guanylate kinase; MARCKS, myristoylated lanine-rich C-kinase substrate; Ncad, N-cadherin; NMDA, N-methyl-D-aspartate; PBCad, PB-cadherin; PDZ, postsynaptic density-95, discs large, ZO-1; PKA, cAMP-dependent protein kinase; PIP₂, phosphatidylinositol-4,5-bisphosphate; PSD, postsynaptic density; SAP97, synapse-associated protein 97.

apses, the PSD is localized to the tip of a dendritic spine opposite the presynaptic active zone releasing glutamate. During LTP, AMPAR recruitment is accompanied by increased spine volume and F-actin polymerization (Matsuzaki *et al.*, 2004; Okamoto *et al.*, 2004). In contrast, LTD decreases spine volume through actin depolymerization (Okamoto *et al.*, 2004; Zhou *et al.*, 2004). Other studies have shown that this spine structural plasticity is interrelated with changes in signaling by transsynaptic adhesion molecules on both sides of the synapse. In particular, cadherins are homophilic calcium-dependent adhesion molecules linked through catenins to F-actin that are important for synapse formation, LTP, and spine structural plasticity (Tang *et al.*, 1998; Bozdagi *et al.*, 2000; Togashi *et al.*, 2002; Okamura *et al.*, 2004).

Here, we report a novel interaction between AKAP79/150 and postsynaptic cadherins. This interaction could further coordinate synaptic form and function by linking components of synaptic adhesion complexes that regulate spine structure with PSD signaling complexes that control receptor activity. Interestingly, we provide evidence for localized assembly of cadherin–AKAP complexes, not only at the PSD of neuronal synapses but also at lateral membrane adherens junctions of epithelial cells. Thus, similar to other studies of neuronal and epithelial polarity, our findings show that AKAP79/150-polarized targeting uses common mechanisms in both cell types. However, our work also indicates that cell-type specific regulation of the AKAP–cadherin interaction by NMDA receptor signaling pathways in neurons could be important for synaptic plasticity mechanisms.

MATERIALS AND METHODS

Yeast Two-Hybrid

Briefly, screens were done in yeast strain L40 harboring *lexA*-regulated HIS3 and *lacZ* reporters. AKAP79 (1-108) and (108-427) cDNA fragments were subcloned into pLexNA. Clones interacting with the LexA(1-108) bait were screened using a rat brain cDNA library (BD Biosciences Clontech, Palo Alto, CA) constructed in Gal4 activation domain vector pACT2. False positives were eliminated by standard methods. To further show specificity of the interaction for (1-108), the remaining pACT2 clones were mated to AMR70 yeast transformed with pLexNA(1-108) as a positive screen and pLexNA(108-427) as a negative screen and scored by β -galactosidase (β -Gal) filter assays. These positive clones were mated to AMR70 yeast transformed with pLexNAAKAP79 as a final secondary positive screen to confirm interaction with full-length AKAP79, and sequenced.

In Vitro Glutathione S-Transferase (GST) Binding Assays

The pGEX (Amersham Biosciences, Piscataway, NJ) vector encoding GST-PBcadCD was constructed by PCR-based *EcoRI*–*Bam*HI subcloning of the PBcadCD from pACT2-PBcad clone #24. GST-PBcadCD truncation and deletion constructs were generated by directed PCR. The pGEX GST-mouse EcadCD vector was provided by Dr. William Weis (Stanford University, Stanford, CA). The pGEX vectors encoding human NcadCD, EcadCD, and EcadCD Δ 1-3 were provided by Dr. Patrick Casey (Duke University, Durham, NC). GST fusion proteins were produced by isopropyl β -D-thiogalactoside induction in *Escherichia coli*, BL21(DE3), lysis by sonication in LB [50 mM Tris, pH 7.5, 0.15 M NaCl, 30 mM NaPPi, 50 mM NaF, 2 μ M Na₃VO₄, 5 mM EDTA, 5 mM EGTA, 2 μ g/ml leupeptin/pepstatin, 1 mM benzamide, 1 mM 4-(2-aminoethyl)benzenesulfonyl fluoride] and purified from cell lysates using glutathione-Sepharose 4B beads (Amersham Biosciences). Bound GST-cad fusion proteins, or ~25 μ g of GST-Ecad Δ 2 and Δ 3, was incubated with 500 ng (~500 nM) of purified AKAP79(1-153)C-His6 (Gomez *et al.*, 2002; provided by Eric Horne, University of Colorado at Denver and Health Sciences Center, Denver, CO), 500 ng (~10 nM) of β -cat (provided by Dr. Patrick Casey), or 5 mg of neonatal rat forebrain for 2 h at 4°C, followed by extensive washing. For the competition assay, increasing amounts of AKAP79(1-153), 50 nM–2.0 μ M (2.0 μ M is 200- and 25-fold molar excesses over β -cat and E-cad, respectively), were incubated in the presence of 10 nM β -cat and 80 nM GST-E-cadCD as described above (reported K_d for Ecad- β -cat interaction is ~10 nM; Roura *et al.*, 1999). Bound protein was eluted by boiling in Laemmli buffer and subjected to SDS-PAGE and immunoblotting (rabbit anti-AKAP79 [1:2000; pro-

vided by Dr. Yvonne Lai, ICOS, Bothel, WA]; mouse anti- β -cat [1:500; BD Transduction Laboratories, Lexington, KY]; mouse anti-GST [1:1000; Santa Cruz Biotechnology, Santa Cruz, CA]). The effects of PKC phosphorylation or calmodulin (CaM) binding were performed as described in Gomez *et al.* (2002).

Immunoprecipitation and Preparation of Synaptosomal Fractions

AKAP150 immunoprecipitations (IPs) from Triton X-100 extracts of Madin-Darby canine kidney (MDCK) cells, hippocampal neurons, and forebrains of P21–P28 Sprague-Dawley rats were performed as per Gomez *et al.* (2002). Immunoblotting of IPs was performed with rabbit anti-AKAP150 (1:2000; provided by Dr. Yvonne Lai), mouse anti-Ncad (1:2000), β -cat (1:500), E-cad (1:2000), and PKA-C (1:500; BD Transduction Laboratories) or pan-anti-PSD-MAGUK (1:1000; Upstate Biotechnology, Charlottesville, VA). Hippocampal neurons cultured at high density on 10-cm poly-D-lysine/laminin-coated dishes for 19–21 d in vitro (DIV) were left untreated or treated with NMDA for 10 min before preparation of cell lysates. Crude synaptosomes were prepared by homogenizing P21–P28 Sprague-Dawley rat forebrains in 5 ml of LB with sucrose followed by a 10-min spin at 1000 \times g at 4°C. Supernatants were centrifuged at 10,000 \times g for 15 min at 4°C. The pellet was either resuspended in TLB for crude synaptosomes (P2) or processed further for preparation of purified synaptosomes (LP1). Briefly, P2 pellets were resuspended in 2 ml of double distilled H₂O, incubated for 30 min on ice and pelleted at 25,000 \times g. Deoxycholate extraction was performed at 37°C with 10% deoxycholate (DOC) in 50 mM Tris, pH 9, followed by dialysis against 50 mM Tris, pH 7.4, and centrifugation at 38,500 \times g. Triton X-100 was shown to efficiently solubilize postsynaptic AKAP150–MAGUK–AMPAR complexes less tightly associated with the PSD, whereas DOC allows additional solubilization of AKAP150–MAGUK–NMDAR complexes more tightly associated with the PSD (Colledge *et al.*, 2000).

Mammalian cDNA Expression Vectors

The pEGFPN1 (BD Biosciences Clontech) vectors encoding C-terminal green fluorescent protein (GFP) fusions of AKAP79, (1-153), (1-108), (75-153), (1- Δ B-153), and (108-427) were described in Dell'Acqua *et al.* (1998). pECFPN1-AKAP79, pEYFPN1-AKAP79, pECFPN1-(1-153), pEYFPN1-(1-153), pEYFPN2-CaNA α , and pEYFPN3-RII α were described in Gomez *et al.* (2002) and Oliveria *et al.* (2003). Vectors encoding N-terminal cyan fluorescent protein (CFP) fusions of AKAP79 and (1-153) were generated in pECFPN3 (BD Biosciences Clontech) using 5' *Hind*III and 3' *Bam*HI cloning sites. The Ncad-yellow fluorescent protein (YFP) C-terminal fusion vector was constructed in pEYFN1 by PCR amplification of the Ncad cDNA sequence (provided by Dr. Deanna Benson, Mt. Sinai Medical Center, New York, NY) adding 5' *Xho*I and 3' *Eco*RI restriction sites. The PSD-95-CFP C-terminal fusion vector was constructed in pECFPN1 by transfer of the PSD-95 cDNA sequence from pEGFPN1-PSD-95 (provided by Dr. Alaa El-Husseini, University of British Columbia, Vancouver, British Columbia, Canada) using 5' *Hind*III and 3' *Eco*RI cloning sites. pCDNA3-AKAP150 was provided by Dr. Naoto Hoshi (Howard Hughes Medical Institute, Oregon Health Sciences University, Portland, OR).

Preparation and Transfection of Primary Hippocampal Neurons

Primary hippocampal neurons were prepared from Sprague-Dawley neonatal rats (P0–P1) as described in Gomez *et al.* (2002). For immunocytochemistry, neurons were plated at low density (15–30,000 cells/ml) and grown 19–21 DIV. For Amaxa transfection experiments, neurons were resuspended at 150,000–250,000 cells/transfection in Amaxa buffer and electroporated with 4–8 μ g of DNA per construct as per manufacturer's protocol (Amaxa, Cologne, Germany) and grown to 13–15 DIV.

Caco-2 and MDCK Cell Culture and Transfection

Caco-2 cells were grown to confluence on collagen-coated glass coverslips and allowed to polarize 14 d in DMEM, 20% fetal bovine serum (FBS), 1% penicillin/streptomycin (Invitrogen, Carlsbad, CA). MDCK type II cells were grown on collagen-coated glass coverslips to 90% confluence in DMEM, 10% FBS, 1% penicillin/streptomycin before transfection with Lipofectamine 2000 with cDNA constructs as per manufacturer's recommendations (Invitrogen). Transfected cells were grown 48–72 h before pharmacological treatment or immunostaining. For experiments in Figures 4 and 5, MDCK cells were grown on Transwell filters (Costar, Cambridge, MA) and transfected at 50–75% confluence using Lipofectamine Plus with cDNA constructs as per manufacturer's recommendations (Invitrogen). Transfected cells on filter inserts were allowed to grow to confluence and polarize for 7 d. Latrunculin A (Molecular Probes, Eugene, OR) and cytochalasin D (EMD Biosciences–Calbiochem, San Diego, CA) treatments were done for 4 h. Calcium switch experiments were done as described previously (Kartenbeck *et al.*, 1991). For AKAP150 immunoprecipitations, MDCK cells were transfected on 10-cm plates 48–72 h before treatments and preparation of cell lysates.

Immunocytochemistry

Hippocampal neurons and epithelial cells were processed for immunocytochemistry as described previously (Gomez *et al.*, 2002). Polyclonal antibodies against AKAP150 (1:2000), AKAP79 (1:1000), and Synaptophysin (1:500; Santa Cruz Biotechnology), and monoclonal antibodies against PSD-95 (1:100; Affinity BioReagents, Golden, CO), SAP97 (1:500; Stressgen Biotechnologies, Victoria, British Columbia, Canada), pan-PSD-MAGUK family, Ncad, Ecad, (1:1000), β -cat (1:500; BD Transduction Laboratories), Ezrin and ZO-1 (1:250; Zymed Laboratories, South San Francisco, CA) were used. In Caco-2 and MDCK cells, similar results were obtained for staining with pan-anti-PSD-MAGUK (Upstate Biotechnology) and anti-SAP97 (Stressgen Biotechnologies) consistent with SAP97 being the only PSD-95 family member expressed. F-actin was stained with Texas Red-phalloidin (1:500). Secondary antibodies conjugated to fluorescein isothiocyanate (1:500), Alexa-488 (1:500), Texas Red (1:250), and Alexa-654 (1:500) and ProLong mounting medium obtained from Molecular Probes.

Fluorescence Microscopy and Quantitative Digital Image Analysis

Live cell imaging of neurons and MDCK cells was performed on an inverted Zeiss Axiovert 200M with 100 \times plan-apo/1.4 numerical aperture (NA) objective, 175-W xenon illumination, Coolsnap charge-coupled device camera, and Slidebook 4.0 software (Intelligent Imaging Innovations, Denver, CO). Samples were maintained at 33°C and ~5% CO₂ during the entire imaging period. For detection of indirect immunofluorescence, three-dimensional z-stacks of xy planes with 0.5- μ m steps were collected for the entire cell imaged. Images were deconvolved to the nearest neighbor to generate confocal xy sections. In Figures 8 and 9A, two-dimensional xy projection images of the entire deconvolved z-stack are shown to better represent a complete picture of dendrites and spines. These projection images also were used for quantitative mask analysis (see below). For Figures 4 and 5, a Zeiss Axiovert 100 microscope with 63 \times plan-apo/1.2 NA objective and a Bio-Rad (Hercules, CA) MRC1024 laser confocal system was used to acquire z-stacks of xy planes with 1.0- μ m spacing or to acquire single xz line-scan sections for a given y location.

Quantitation of fluorescence signals in hippocampal neurons was done as described in Gomez *et al.* (2002). Dendrite/soma ratio measurements were achieved by drawing masks to the entire dendritic tree and to the soma using the segmenting function of Slidebook. Results are presented as mean fluorescence intensity ratios. Measurements of colocalization were achieved by generating segmented dendritic puncta masks showing discrete areas of continuous pixels of fluorescence intensity >100% above the mean dendritic fluorescence for AKAP150, Ncad, β -cat, PSD-95, and synaptophysin (Syp). A second mask containing only colocalized integrated intensity signal per pairing was generated using the "AND" function. This colocalized signal was then normalized to the integrated intensity value of the marker, which was PSD-95, Ncad, β -cat, or Syp, depending on the experiment. Fluorescence micrograph images were exported as RGB TIFF files and assembled into figures using Adobe Photoshop 5.5–7.0.

Fluorescence Resonance Energy Transfer (FRET) Microscopy

For FRET analysis, transfected MDCK grown on 25-mm round coverslips cells were placed in a chamber (Molecular Probes) for live cell imaging of intrinsic YFP or CFP fluorescence as detected in single focal planes. Two methods to obtain FRET information were used. The first method, "microFRET," relied on capturing three images: 1) YFP excitation/YFP emission; 2) CFP excitation/CFP emission; and 3) CFP excitation/YFP emission (raw FRET) and then fractional image subtraction to correct for both CFP bleed-through (0.55), YFP cross-excitation (0.016) and background in raw FRET images to yield FRETc images. The second method, YFP acceptor photobleaching, directly measured the dequenching of CFP emission after the YFP acceptor was bleached (535 nm for 2 min). This FRET was expressed as the postbleach CFP minus the prebleach CFP as a fraction of the postbleach CFP or apparent FRET efficiency = $\Delta\text{CFP}/\text{CFP}_{\text{post}}$. Mean intensity values used to calculate FRETnc (FRETc/CFP \times YFP $\times 10^5$) for microFRET and apparent FRET efficiencies from YFP photobleaching were obtained by mask analysis in Slidebook as described previously (Oliveria *et al.*, 2003).

RESULTS

Identification of an Interaction between AKAP79 and Cadherins

AKAP79/150 targeting to dendritic spines depends on its N terminus (1-153), which is comprised of three basic domains. Each domain is similar to the effector domain of myristoylated-alanine-rich C kinase substrate (MARCKS) and binds F-actin and acidic lipids such as phosphatidylinositol-4,5-

bisphosphate (PIP₂) (Dell'Acqua *et al.*, 1998; Gomez *et al.*, 2002). Although PIP₂ and actin are enriched at spines, we reasoned that interactions with other proteins might participate in targeting the AKAP to the PSD. To this end, a yeast two-hybrid screen of a rat brain cDNA library was conducted using as bait AKAP79(1-108) that contains two of the three basic domains and is sufficient for dendritic membrane targeting (Figure 1A). To eliminate proteins that nonspecifically bind basic regions, clones were further screened for interaction with full-length AKAP79 and for lack of interaction with (108-427) that contains a single basic domain and does not target to membranes (Figure 1A). This screening identified three clones for rat PB-cadherin (PBCad) (Sugimoto *et al.*, 1996) (Figure 1, B and C). No other classical cadherins were found in this screen; however, identification of transmembrane proteins is rare in two-hybrid screens. All three PBCad clones contained the intact cytoplasmic domain (CD), including the conserved β -cat binding site with truncations of the extracellular domain that engages in homophilic adhesion (Figure 1B). These cloning results point to the CD as the site of AKAP79 interaction.

The AKAP79 N-Terminal Basic Domains Bind to a Conserved Acidic Region within the β -Catenin Binding Site of Cadherins

Confirming our two-hybrid results, AKAP79(1-153) bound *in vitro* to GST-PBCadCD but not GST alone (Figure 1F). AKAP79(1-153) also bound to Ecad and Ncad CD with cadherin binding to β -cat as a positive control (Figure 1D). Using truncations and deletions of PBCad, the AKAP79 interaction site was mapped to residues 735-761 (Figure 1, E and F) that contain charged and acidic regions conserved in Ecad and Ncad (Figure 1I). Further analysis of (1-153) binding to human Ecad deletions narrowed the site of interaction to the acidic region 819-837 defined by Ecad Δ 2 (Figure 1, E-F, and I). Interestingly, this cadherin region also is necessary for β -cat binding and cell adhesion (Huber and Weis, 2001; Kaplan *et al.*, 2001). We therefore wanted to address whether AKAP binding might compete with β -cat binding to Ecad. Even when AKAP79(1-153) was present at ~25-fold excess over Ecad and 200-fold excess over β -cat, AKAP79(1-153) displayed saturable binding to GST-Ecad without displacement of bound β -cat, suggesting that *in vitro*, AKAP binding does not preclude binding of β -cat to Ecad (Figure 1J).

Interactions of the three AKAP79 basic domains with PIP₂ and F-actin are disrupted by PKC phosphorylation or Ca²⁺-CaM binding through an electrostatic switch mechanism similar to that seen with the MARCKS basic effector domain (McLaughlin and Aderem, 1995; Dell'Acqua *et al.*, 1998; Gomez *et al.*, 2002). In addition, Ecad binding to β -cat depends in part on electrostatic interactions between acidic cadherin and basic catenin residues (Huber *et al.*, 2001). Accordingly, *in vitro* phosphorylation of (1-153) by PKC prevented coprecipitation with GST-PBCad, as did preincubation with Ca²⁺-CaM (Figure 1G). However, when Ca²⁺ was chelated with EGTA, (1-153) binding to PBCad was unaffected by CaM (Figure 1G). Confirming a requirement for electrostatic interactions, GST-EcadCD precipitation of (1-153) was decreased (24–57%) by increasing NaCl concentration (250–1000 mM; Figure 1H). Overall, these findings suggest that the same basic regions within the AKAP79 targeting domain that interact with acidic lipids and F-actin also are important for binding acidic cadherin cytoplasmic domains.

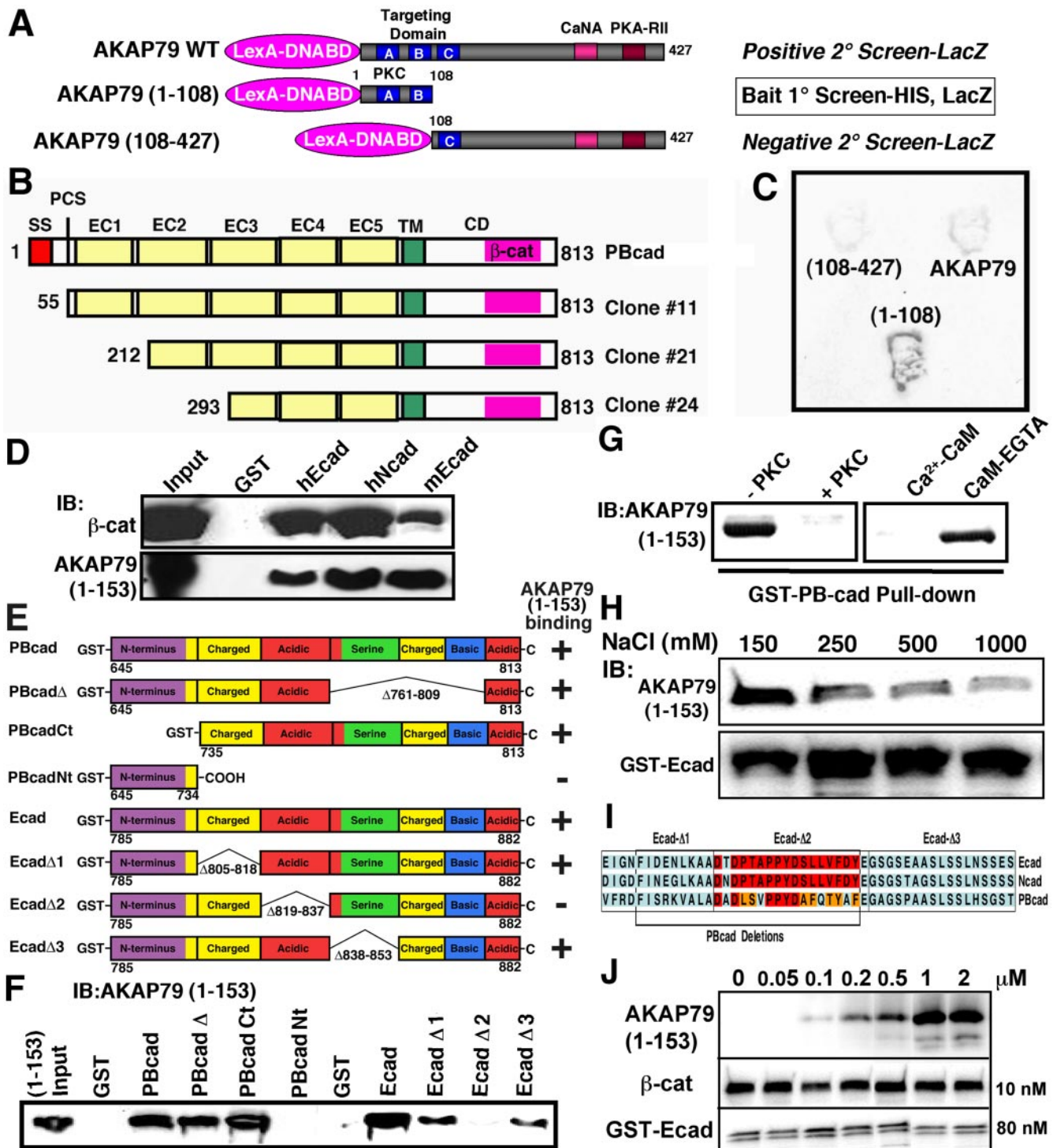
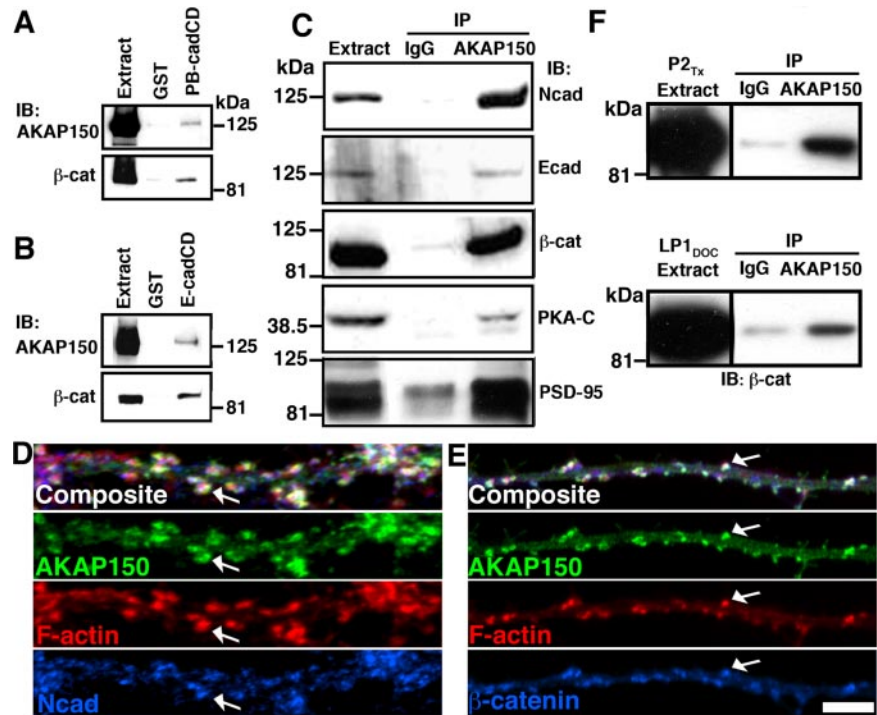


Figure 1. Identification of an interaction between AKAP79/150 and cadherins. (A) Diagram showing the AKAP79 baits used in positive [AKAP79(1-108) and AKAP79WT] and negative [AKAP79(108-427)] yeast two-hybrid screens of a rat brain cDNA library. Locations of three basic regions (A–C) within the targeting domain and PKC-, CaNA-, and PKA-RII-anchoring sites are indicated. (B) Primary structures of Gal4-cDNA PBCad clones identified as interacting with the AKAP79(1-108) bait. The extracellular domain (EC), transmembrane domain (TM), cytoplasmic domain (CD), signal sequence (SS), proteolytic cleavage site (PCS), Ca²⁺-adhesion repeats (EC1–5), and β -cat are indicated. (C) Representative yeast two-hybrid β gal filter assays for interactions of the indicated baits with PBCad Clone#24. (D) Five hundred nanograms of purified AKAP79(1-153)-His6 tagged fragment or β -cat was assayed for cadherin CD binding in vitro by precipitation with 5 μ g of GST (negative control) and 5 μ g of GST-CD fusions for human Ecad (hEcad) and Ncad (hNcad) and mouse Ecad (mEcad) followed by immunoblotting (IB). (E) Diagram showing the primary structures of PBCad and Ecad deletions used to map the AKAP79 binding site (not to scale). Previously delineated (Kaplan *et al.*, 2001) subregions within the cadherin CD that are rich in charged, acidic, serine, or basic residues are indicated. AKAP79(1-153) binding results (shown in F) are summarized by a + or – sign. (F) Representative immunoblots showing AKAP79(1-153) binding activity for the PBCad and Ecad-CD constructs diagrammed in E. GST-fusion constructs were present at equal levels

Figure 2. AKAP79/150, cadherins, and β -catenin are present in neuronal postsynaptic complexes. Isolation of endogenous AKAP150 and β -cat from 5 mg of rat brain extracts through binding to 5 μ g of GST-PBcadCD (A) and 5 μ g of GST-EcadCD (B). (C) Isolation of cadherins and β -cat by immunoprecipitation (IP:) with AKAP150 from 5 mg of rat brain extracts. Five micrograms of anti-AKAP150 or IgG (nonimmune, negative control) IPs was analyzed by immunoblotting (IB:) as indicated. (D) Postsynaptic dendritic spine colocalization (arrows, white in composite panels) of AKAP150 (green) with F-actin (red) and Ncad (blue) or (E) β -cat (blue) in dendrites of hippocampal neurons. (F) Isolation of β -cat in complexes with AKAP150 from rat brain synaptic membranes. AKAP150 or IgG IPs of \sim 500 μ g of Triton X-100-solubilized crude synaptosomes (P2_{Tx}) or DOC-extracted purified synaptosomes (LP1_{DOC}) were analyzed for β -cat by IB. Bar, 5 μ m.



Isolation of Complexes Containing AKAP79/150, Cadherins, and β -Catenin from Rat Brain

To determine whether AKAP79/150 and cadherins form complexes under more physiological conditions, we first pulled down endogenous AKAP150 and β -cat from rat brain with GST-PBcad and Ecad (Figure 2, A and B). Next, antibodies to AKAP150 were used to coprecipitate Ncad and Ecad (Figure 2C). β -cat also was detected in these AKAP150 precipitates, further suggesting that the AKAP and β -cat may be able to bind to same cadherin molecules despite overlapping binding sites. Positive controls demonstrated that AKAP150 antibodies precipitated PSD-95 MAGUKs and PKA, known AKAP150 binding partners (Figure 2C). In cultured hippocampal neurons, punctate colocalization (white) of AKAP150 and F-actin with either Ncad or β -cat (Figure 2, D and E) was seen in postsynaptic dendritic spines. Some staining for Ncad and β -cat that is opposed to spines but nonoverlapping with AKAP150 and F-actin was seen, as expected for localization of Ncad and β -cat to presynaptic terminals. To confirm that AKAP–cadherin–catenin complexes exist at synapses, we immunoprecipitated

β -cat with AKAP150 from two different rat brain synaptic membrane preparations (Figure 2F).

Localization of AKAP79 with Cadherins and β -Catenin at Epithelial Adherens Junctions

The synaptic junction shares many similarities with the lateral adherens junction of epithelial cells. In both structures cadherins are associated with β -cat, which links to the actin cytoskeleton through association with α -catenin (α -cat) (reviewed in Pokutta and Weis, 2002). In addition, PDZ–MAGUK complexes play central roles in coordinating epithelial (apical vs. basolateral) and neuronal (axonal vs. somato-dendritic) polarity and junctional assembly of signaling complexes (Bredt, 1998). Importantly, the PSD-95 family MAGUK SAP97 (rat SAP97; Drosophila and human Discs large [hDlg]), that binds AKAP79/150 and links it to synaptic AMPARs, also is present at epithelial adherens junctions (Lue *et al.*, 1996; Reuver and Garner, 1998). Immunoblotting of Caco-2 cells, a human colonic carcinoma epithelial cell line, detected expression of AKAP79 as well as Ecad, β -cat, and SAP97 (our unpublished data). Caco-2 immunostaining revealed AKAP79 localization to lateral membranes with Ecad, β -cat, F-actin, and SAP97 (Figure 3, C–E, and 3C'–E'). Although AKAP79 staining was strongest in lateral membranes, some localization was seen in more basolateral sections (Figure 3, A–E). In contrast, AKAP79 staining was not apparent in apical sections and did not colocalize with apical ezrin or tight junction ZO-1 (Figure 3, A and B, and A' and B'). AKAP79's colocalization with actin was restricted to lateral membranes and was not seen in apical microvilli or basolateral stress fibers (Figure 3, E and E').

Like endogenous AKAP79 in Caco-2 cells, xy confocal microscopy detected transfected AKAP79-GFP in MDCK epithelial lateral and basolateral but not apical membranes (Figure 4E). AKAP79-GFP fluorescence overlapped well with Ecad and β -cat in lateral membranes (Figure 4, C and

Figure 1 (cont). (5 μ g), except Ecad- Δ 2 and Ecad- Δ 3 were present at fivefold higher levels, suggesting reduced binding for Ecad- Δ 3. (G) PKC phosphorylation or preincubation of 1 μ g of AKAP79(1-153) with 1 μ M Ca^{2+} -CaM, but not CaM plus EGTA, prevented GST-PBcad pull-down. (H) High salt concentrations (250–1000 mM) inhibit AKAP79(1-153) binding to GST-Ecad. (I) Amino acid sequence alignment of human Ecad, Ncad, and rat PBcad showing regions within the β -cat binding domain that are necessary for AKAP79 binding. Identical residues are shown in red and conservative substitutions in orange. (J) Immunoblots showing saturable binding of AKAP79(1-153) (0.05–2 μ M) to a fixed amount of GST-Ecad (80 nM) with equal amounts of β -cat (10 nM). Both AKAP79(1-153) and β -cat are pulled down, even in the presence of a large molar excess of AKAP present (\sim 200-fold over β -cat).

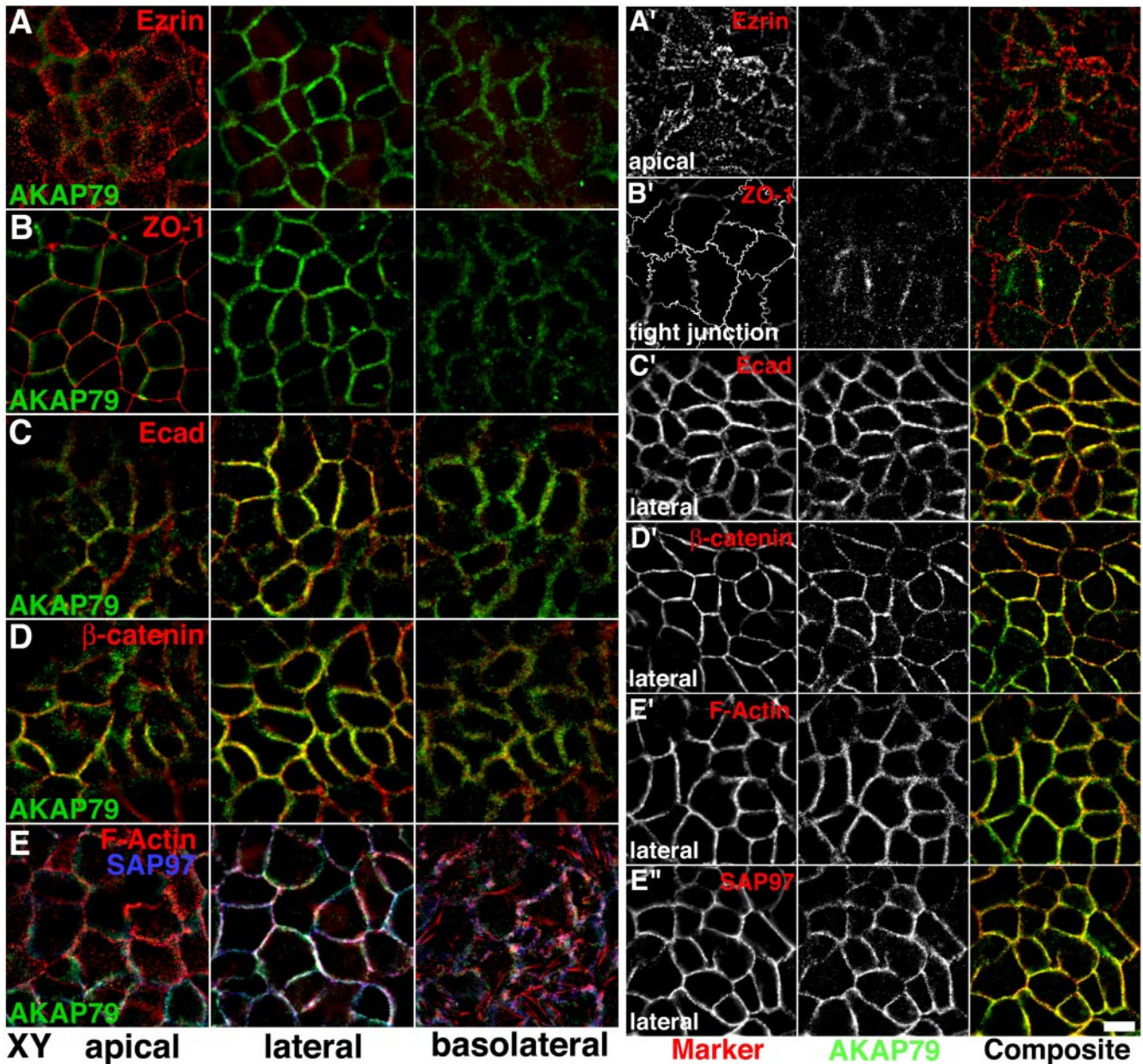


Figure 3. Polarized localization of endogenous AKAP79 with E-cadherin at the lateral membrane adherens junctions of Caco-2 epithelial cells. Lack of colocalization of AKAP79 (green) with apical membrane ezrin (red) (A and A') and tight junction ZO-1 (red) (B and B'). Lateral membrane colocalization (yellow) of AKAP79 (green) with Ecad (red) (C and C') and β -cat (red) (C and C'). (E, E', and E'') Lateral membrane colocalization (white or yellow) of AKAP79 (green) with cortical F-actin (red, E and E') and SAP97 (E, blue; E'', red). (A-E) xy, composite images through apical, lateral, and basolateral membranes as labeled. (A'-E'') Individual channels and composite images for a single xy section through apical, lateral, and basolateral membranes as labeled. Bar, 10 μ m.

D), but it showed little overlap with ZO-1 or ezrin in more apical sections (Figure 4, A and B). The corresponding xz scans clearly demonstrated AKAP79-GFP lateral membrane colocalization with Ecad and β -cat and lack of localization with tight junction ZO-1 and apical ezrin (Figure 4, A-D). Similar to AKAP79-GFP, AKAP150 localized with Ecad in MDCK lateral membranes (Figure 4F). To confirm that AKAP lateral localization corresponds with assembly into complexes with cadherin, catenins, and MAGUKs, we precipitated Ecad, β -cat, and SAP97 with AKAP150 but not nonimmune IgG (Figure 4G).

Polarized Targeting of AKAP79 to Epithelial Lateral Membranes Is Mediated by the Three N-terminal Basic Domains

GFP-fusion proteins with deletions in the AKAP79 targeting domain were expressed in MDCK cells (Figure 5F). The intact N-terminal domain (1-153) targeted GFP to the lateral membrane, below ZO-1 at the tight junction (Figure 5A). Three additional fragments [(1-108), the fragment used as bait in the two-hybrid screen; (75-153); and (1- Δ B-153)] that cover all possible combinations of two of the basic domains were each sufficient to confer lateral membrane targeting,

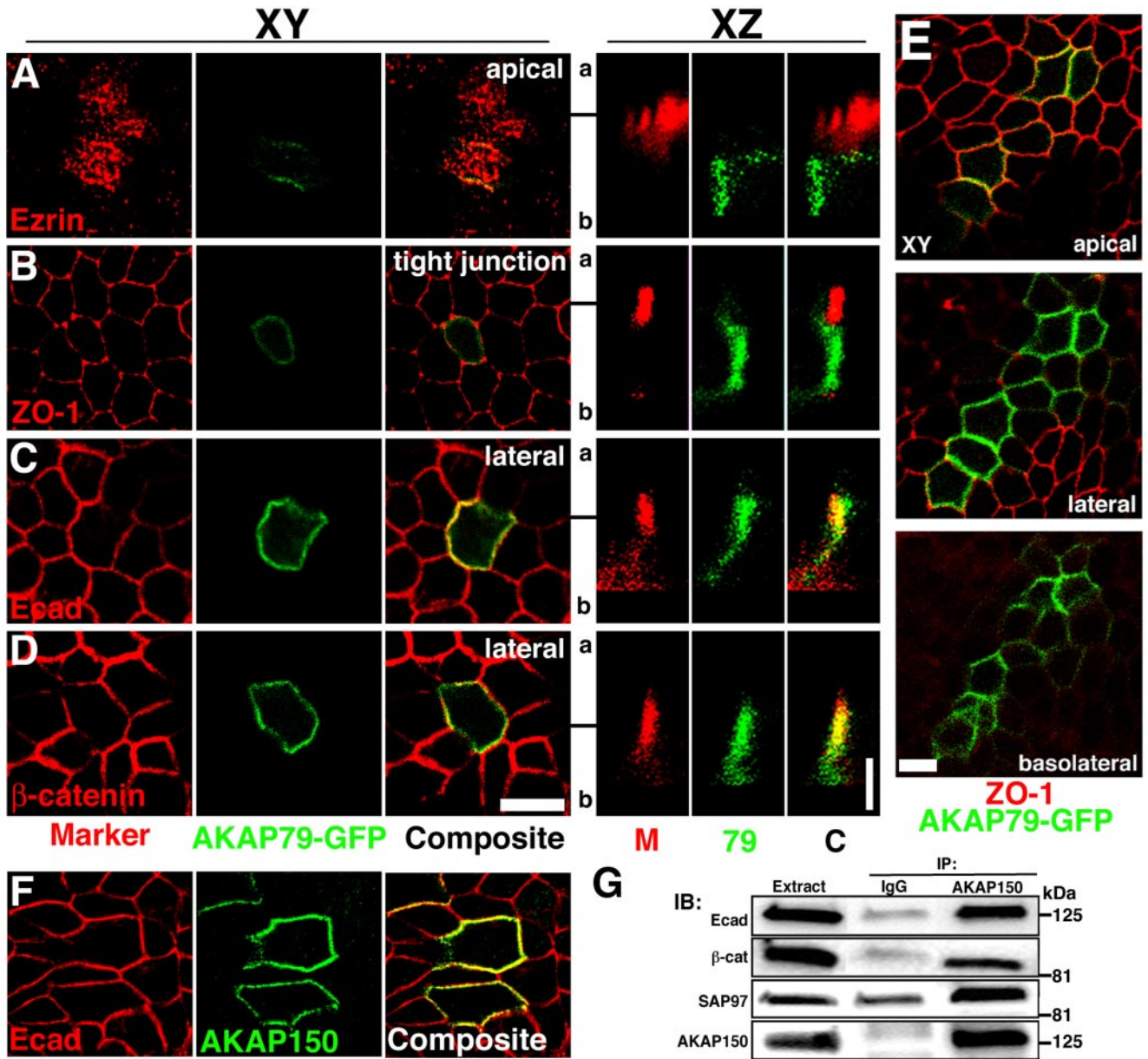


Figure 4. Polarized localization of AKAP79-GFP and association of AKAP150 with E-cadherin at lateral membranes of MDCK epithelial cells. Lack of colocalization of AKAP79-GFP (green) with apical marker ezrin (79, red) (A) and tight junction marker ZO-1 (M, red) (B). Colocalization (yellow) of AKAP79-GFP (79, green) with lateral membrane Ecad (M, red) (C) and β -cat (M, red) (D). (A–D) Right-hand panels show vertical xz line-scan sections from apical (a) to basolateral (b) for the same cells shown in the left-hand xy panels (y location in xy plane relative to the xz scan is indicated by a black line). (E) Apical, lateral, and basolateral xy sections showing AKAP79-GFP (green) basolateral membrane localization relative to tight junction ZO-1 (red). (F) Lateral membrane (xy) colocalization (yellow) of AKAP150 (green) with Ecad (red). (G) Coimmunoprecipitation of Ecad, β -cat, and SAP97(hDlg) with 5 μ g of anti-AKAP150 but not nonimmune IgG from \sim 3 mg of transfected MDCK cell lysates. Bars, 10 μ m for xy sections, 5 μ m for xz sections. Note: We are unable to detect expression of any endogenous canine AKAP protein with our antibodies to human AKAP79 or rat AKAP150.

below ZO-1 at the tight junction (Figure 5, B–D). However, a C-terminal fragment (108–427) that contains a single basic domain (negative control in the two-hybrid screen) did not show membrane targeting and was diffuse and cytoplasmic (Figure 5E). These results are consistent with our analyses of these fragments for polarized targeting in neuronal dendrites (Dell’Acqua *et al.*, 1998) and demonstrate that fragments with cadherin binding activity also exhibit polarized targeting to epithelial lateral membranes.

FRET Imaging of PKA and CaN Anchoring to AKAP79 at the Lateral Membrane of Living Epithelial Cells

We next characterized interactions of AKAP79 with cadherins, PKA-RII regulatory subunit dimer, and CaNA catalytic subunit in living epithelial cells using FRET microscopy (Oliveria *et al.*, 2003). FRET involves the nonradiative transfer of energy from a donor fluorophore (CFP) to an acceptor fluorophore (YFP). Energy transfer only occurs when the donor and acceptor fluorophore dipoles are in favorable

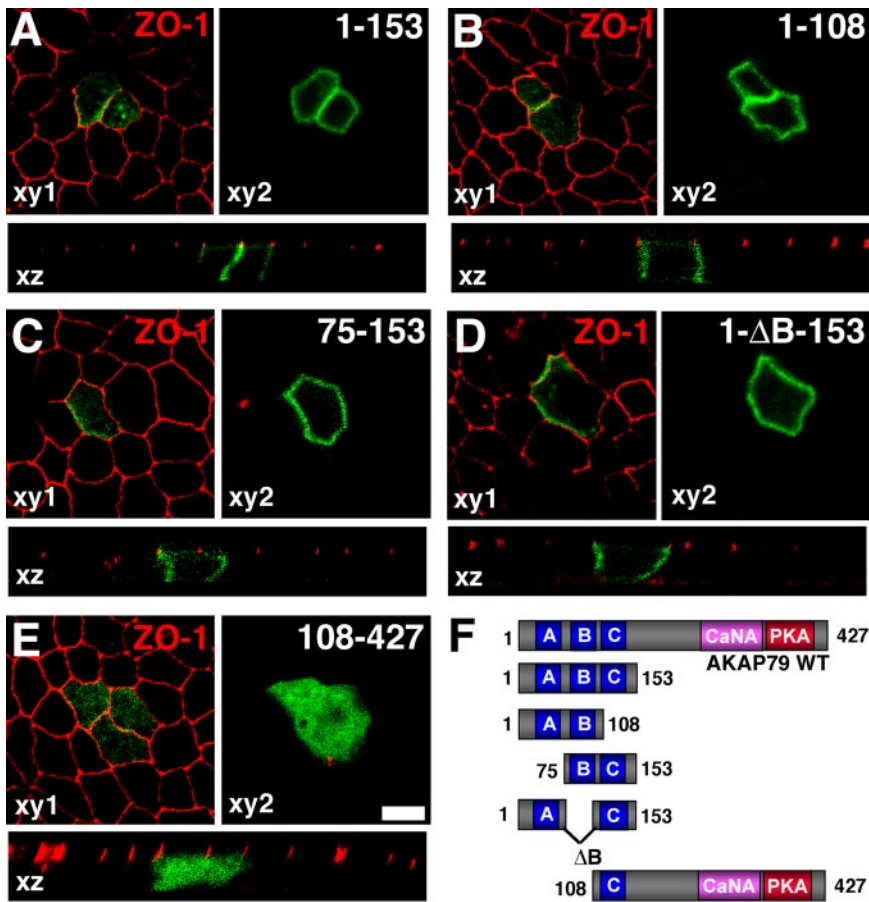


Figure 5. The three basic regions within the AKAP79 N-terminal targeting domain mediate polarized localization to MDCK lateral membranes. (A) AKAP79(1-153)-GFP (green) containing all three (A–C) basic regions, (B) AKAP79(1-108)-GFP (green) containing the first two (A and B) basic regions, (C) AKAP79(75-153)-GFP (green) containing the second two (B and C) basic regions and (D) AKAP79(1- Δ B-153)-GFP (green) containing the first and the third (A and C) basic targeting regions all localize to MDCK lateral membranes (xy2 plane) but not to ZO-1 (red) expressing tight junctions (xy1 plane). The transverse plane (xz) shows a lack of colocalization of AKAP constructs (green) with the tight junction marker ZO-1 (red). (E) AKAP79(108-427)-GFP containing a single (C) basic region fails to show membrane localization. (F) Diagram showing primary structures of AKAP79-GFP fragments used in A–E. Bar, 10 μ m.

mutual orientation and are no further apart than ~ 50 Å. Imaging of both a C-terminally tagged AKAP79 (AKAP79ct-CFP) and an N-terminally tagged AKAP79 (CFP-AKAP79nt) with either PKA-RII-YFP or CaNA-YFP revealed good colocalization at the lateral membranes (Figure 6, A and B, composite panels). However, positive FRET signals were only observed with the C-terminally tagged AKAP constructs, shown either as FRETc signal gated to CFP donor (Figure 6, A and B, FRETc/CFP panels) or as corrected FRET (Figure 6, A and B, FRETc panels). Calculation of normalized FRETc (see *Materials and Methods*) values demonstrated lateral membrane FRET for AKAP79ct-CFP with RII-YFP (8.6 ± 0.7) and CaNA-YFP (13.6 ± 2.7). Lack of FRET for CFP-AKAP79nt with RII-YFP and CaNA-YFP was demonstrated by low FRETc values (0.5 ± 1.4 and 0.3 ± 0.9 , respectively; Figure 6E). These positive FRET interactions between AKAP79ct-CFP and RII-YFP and CaNA-YFP were confirmed by YFP photobleaching measurements of apparent FRET efficiencies (see *Materials and Methods*) of 5.3 ± 0.4 and $4.1 \pm 0.8\%$, respectively (Figure 6E). In contrast, lack of FRET for CFP-AKAP79nt with PKA and CaN was indicated by apparent FRET efficiencies of only 1.2 ± 0.7 and $0.8 \pm 1.0\%$ (Figure 6E). Thus using both methods of FRET analysis, we were only able to detect FRET between PKA or CaN with a C-terminally tagged AKAP79, consistent with the binding site for these enzymes being close to the C terminus of AKAP79.

Given our FRET results for AKAP79 with PKA and CaN that bind near the AKAP C terminus, we reasoned that AKAP-cadherin interactions might be optimally detected with the CFP-AKAP79nt, due to the localization of cadherin

binding to the N terminus. Although, expression of CFP-AKAP79nt or CFP-(1-153)nt with Ncad-YFP (tagged at the CD C terminus) yielded good lateral membrane colocalization (Figure 6, C and D), no FRETc was detected (our unpublished data) and apparent FRET efficiencies obtained from YFP photobleaching experiments were only 1.8 ± 0.6 and $1.5 \pm 0.4\%$, respectively (Figure 6E). Similar results were obtained when AKAP79 or (1-153) was labeled at the C terminus (our unpublished data). Thus, lack of robust FRET for the AKAP-cadherin interaction suggests that the fluorophores are either too far separated or not oriented favorably in the complex. Nonetheless, our positive FRET measurements suggest that AKAP79 recruits both PKA and CaN to cell adhesions.

Lateral Membrane Localization of AKAP79 Depends on F-Actin and Is Regulated by Cadherin Adhesion

Localization of AKAP79 to neuronal dendritic spines depends on the actin cytoskeleton (Gomez *et al.*, 2002). Numerous studies have shown that tethering of cadherin-catenin complexes to cortical actin stabilizes adherens junctions (Pokutta and Weis, 2002). MDCK cells transfected with AKAP79-GFP were treated with latrunculin A to inhibit actin polymerization and disrupt lateral membrane F-actin staining (Figure 7B). Latrunculin caused decreased lateral membrane localization and an increase in intracellular localization for AKAP79-GFP (Figure 7A). In agreement with previous studies (Reuver and Garner, 1998), SAP97 staining also became disorganized and more intracellular upon actin depolymerization (Figure 7B). As expected, signal for Ecad also was disorganized, dissociated from lateral membranes,

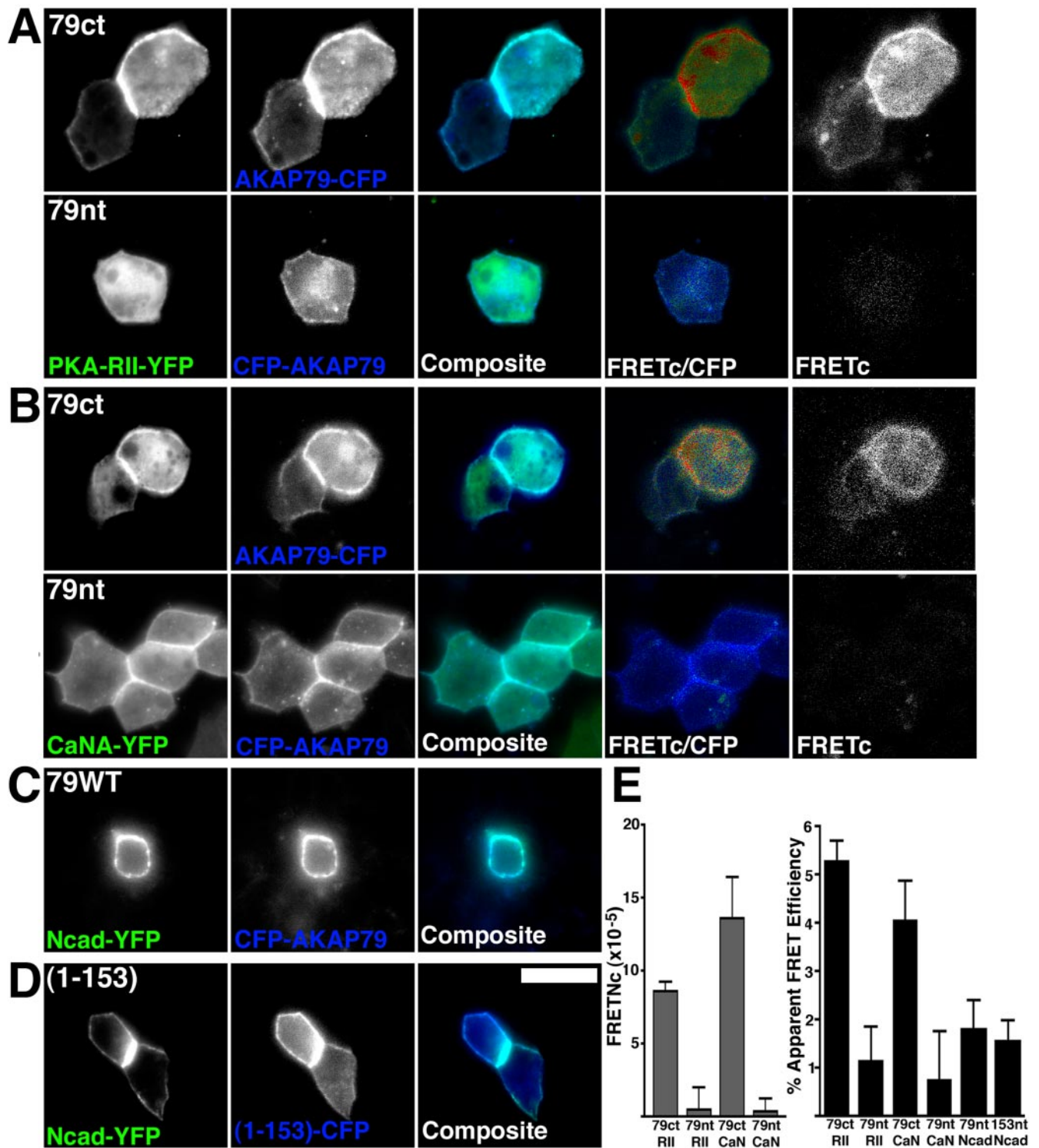


Figure 6. Lateral membrane localization with Ncad and anchoring of PKA and CaN to AKAP79 imaged in living MDCK cells. FRET imaging of PKA-RII-YFP (green) (A) or CaNA-YFP (green) (B) anchoring to AKAP79-CFP (blue) at MDCK lateral membranes with a C-terminal (79ct) but not N-terminal (79nt) CFP chromophore. In A and B, FRETc (see *Materials and Methods*) is shown both in monochrome (far right) and as a CFP donor-gated image (FRETc/CFP) that represents relative FRET signal intensity on a pseudocolor scale of no FRET, blue; low FRET, green; and high FRET, red. Lateral membrane colocalization of Ncad-YFP with CFP-AKAP79 (C) and AKAP79(1-153)-CFP (D) in living MDCK cells. No FRETc was detected in C and D (our unpublished data). (E) Normalized mean FRETc (FRETNC \pm SEM; see *Materials and Methods*) calculated from multiple FRETc images for AKAP79 anchoring of PKA-RII and CaN (left-hand graph). Apparent mean FRET efficiencies (\pm SEM) measured from YFP-acceptor photobleaching (see *Materials and Methods*) for AKAP79 or AKAP79(1-153)-CFP interactions with PKA-RII, CaN, and Ncad-YFP (right-hand graph). Bar, 10 μ m.

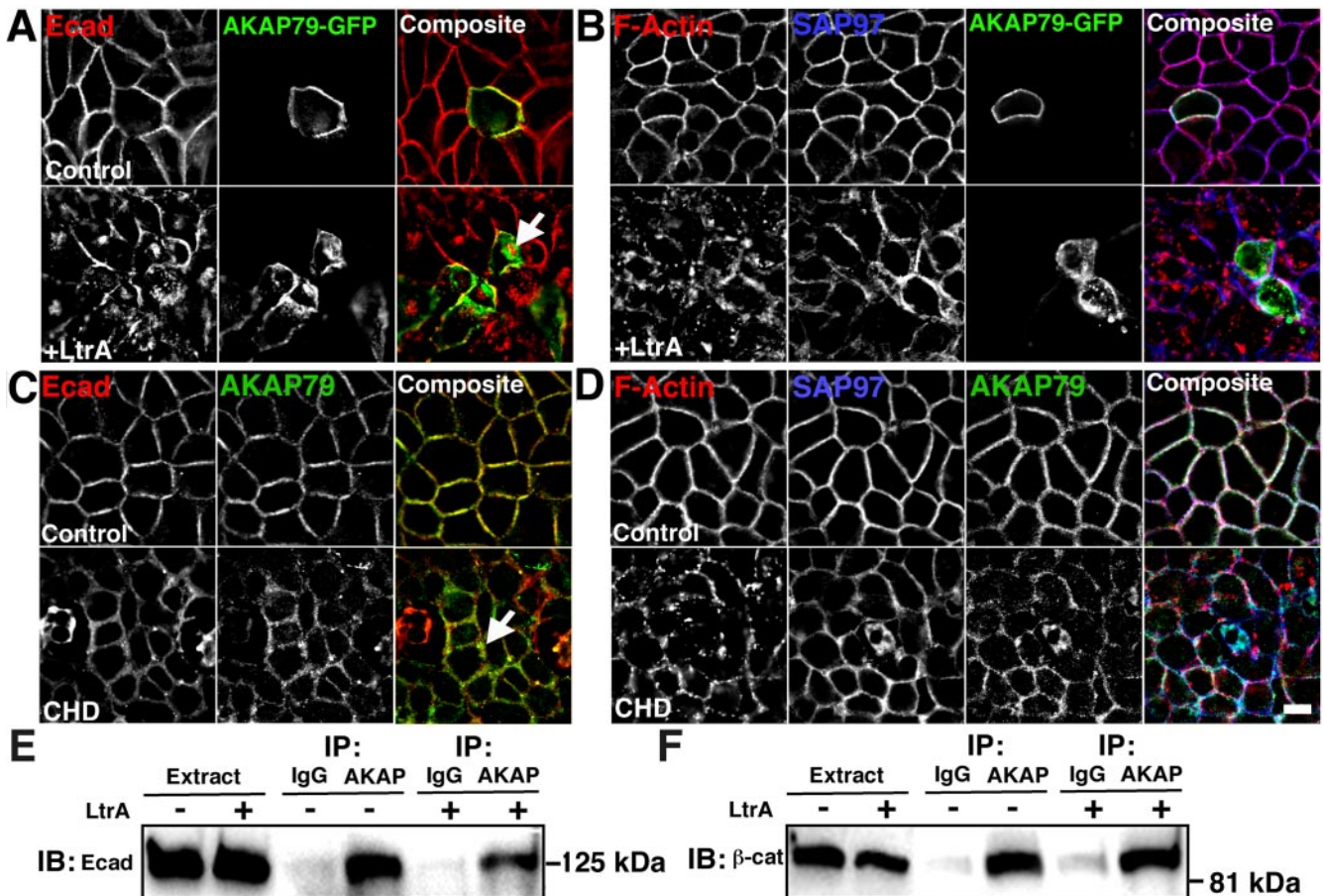


Figure 7. Disruption of the cortical actin cytoskeleton leads to loss of AKAP79 lateral membrane localization in epithelial cells. (A and B) Treatment of MDCK cells with latrunculin A (LtrA, 5 μ M, 4 h) causes loss of lateral membrane localization (yellow or white) of AKAP79-GFP (green) with Ecad (red) (A) and F-actin (red), SAP97 (blue) (B). (C and D) Treatment of Caco-2 cells with cytochalasin D (CHD, 5 μ M, 4 h) causes loss of lateral membrane localization of endogenous AKAP79 (green) with Ecad (red) (C), F-actin (red) and SAP97 (blue) (D). Although colocalization of the AKAP with Ecad is reduced by LtrA or CHD depolymerization of actin, some intracellular overlap is still present (yellow, see arrows). (E and F) LtrA does not disrupt anti-AKAP coIP of Ecad (E) or β -cat (F) from approximately 5 mg of AKAP150-transfected MDCK cell lysates. Nonimmune IgG is used as a control for IP specificity. Bars, 10 μ m.

and more intracellular (Figure 7A). Similar results were obtained when Caco-2 cells were stained for endogenous AKAP79 after treatment with another actin inhibitor, cytochalasin D (Figure 7, C and D). In all cases, although actin depolymerization decreased lateral membrane colocalization of AKAP and Ecad, partial colocalization of these proteins was seen in more intracellular locations (Figure 7, A and C, arrows), suggesting that AKAP-cadherin complexes may still be present. To evaluate this possibility, we immunoprecipitated AKAP150 from transfected MDCK cells and found nearly equal AKAP coprecipitation of endogenous Ecad (Figure 7E) and β -cat (Figure 7F) from control untreated versus latrunculin-treated cells. These immunoprecipitation results indicate that actin polymerization is not required for isolation of AKAP-cadherin-catenin complexes, but our microscopy data show that intact cortical F-actin is important for proper localization of AKAP79 and cadherins at cell contacts.

Maintenance of adherens junctions depends not only on linkage to F-actin but also on signals triggered by cadherins that regulate the cytoskeleton through Rho GTPases (Yap and Kovacs, 2003). Despite complex mechanisms underlying these signals, they can easily be blocked by extracellular

Ca^{2+} depletion that disrupts cadherin homophilic interaction. In control extracellular Ca^{2+} , cortical F-actin was intact (Figure 8A, top row), and lateral membrane colocalization was seen for AKAP79-CFP with endogenous Ecad (Figure 8B, top row, yellow). After 1 h at 37°C in low Ca^{2+} , cell-cell adhesion was disrupted and cortical actin was disorganized (Figure 8A, middle row). In these cells, where adhesion was disrupted, AKAP79 and Ecad were delocalized from the plasma membrane to intracellular locations where only partial AKAP-cadherin colocalization remained (Figure 8B, arrows, middle row). After 1 h of recovery in normal Ca^{2+} (Figure 8, A and B, bottom row), cell-cell adhesion was restored and F-actin, AKAP79, and Ecad returned to lateral membranes. In these cells, transfected Ncad-YFP exhibited similar cellular distributions to endogenous Ecad in all three experimental conditions (Figure 8C). Similar to actin depolymerization, AKAP-cadherin-catenin complexes remained intact even when cadherin adhesion was disrupted as seen by equal AKAP150 coprecipitation of Ecad and β -cat (Figure 8D) in control, low Ca^{2+} , and recovered cells, thus suggesting that the AKAP and cadherin may traffic together. Supporting this idea, we observed parallel loss of Ncad-YFP and AKAP79-CFP from lateral membranes and appearance in

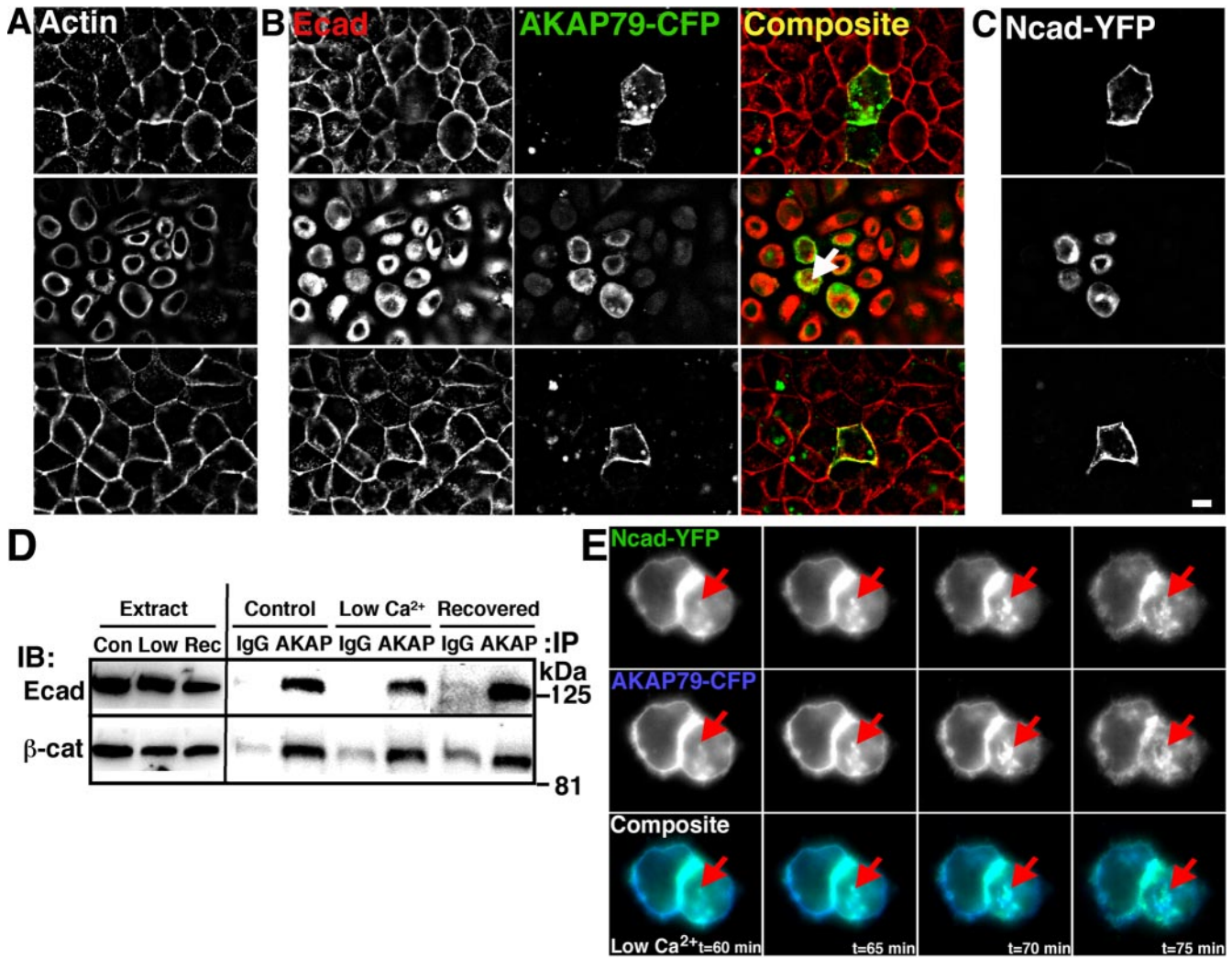


Figure 8. Disruption of cadherin homophilic interactions by low extracellular Ca²⁺ leads to loss of AKAP79 lateral membrane localization in epithelial cells. (A–C) MDCK cells transfected with AKAP79-CFP and Ncad-YFP were imaged under control conditions (top row, 2 mM Ca²⁺), in reduced calcium (middle row, 2 μM Ca²⁺, 1 h), and after recovery (bottom row, 2 mM Ca²⁺, 1 h). (A) F-actin (monochrome, not in composite) lateral membrane localization (control, top row) is lost in low calcium media (middle row) that is restored to pretreatment conditions after 1-h recovery in normal calcium (bottom row). (B) Under control conditions (top row), AKAP79-CFP (green) colocalizes (yellow) with endogenous Ecad (red) at lateral membranes. Despite reduced colocalization of AKAP79-CFP with endogenous Ecad at lateral membranes in low calcium conditions (middle row), some intracellular colocalization is still seen (arrow). AKAP and Ecad lateral membrane localization is restored after 1-h recovery (bottom row). (C) Ncad-YFP (monochrome, not in composite) shows a similar distribution to endogenous Ecad in all experimental conditions. (D) Despite loss of membrane colocalization, inhibition of cadherin adhesion by low Ca²⁺ does not disrupt AKAP coIP of Ecad or β-cat in approximately 5 mg of AKAP150-transfected MDCK cell lysates. Nonimmune IgG is used as a control for IP specificity. (E) AKAP79-CFP (blue) and Ncad-YFP (green) are lost from lateral membranes and occur in common intracellular structures (arrows) over the same time course in living MDCK cells in low Ca²⁺ (t = 60–75 min, 33°C). Bar, 10 μm.

common intracellular structures in live-cell time-lapse imaging done in low Ca²⁺ at 33°C (Figure 8E, arrows). Overall, these findings demonstrate that cadherin signaling to the actin cytoskeleton regulates AKAP79 targeting to cell contacts with cadherins and β-cat.

NMDA Receptor Activation Disrupts Postsynaptic Interaction of AKAP79/150 with Cadherins and β-Catenin

In hippocampal neurons, NMDAR intracellular Ca²⁺ signals that mimic LTD (Beattie *et al.*, 2000) and depolymerize spine F-actin (Halpain *et al.*, 1998) also negatively regulate postsynaptic localization of AKAP79/150 (Gomez *et al.*, 2002). Analysis of NMDA-treated hippocampal neurons

stained for AKAP150, Ncad, or β-cat revealed that endogenous AKAP150 moved away from Ncad and β-cat on spines (Figure 9, A and B, arrows). AKAP150's dendritic membrane localization was decreased, and its appearance in the soma cytoplasm was increased (~50% decrease in dendrite/soma fluorescence ratio, *p < 0.001; Figure 9C). In contrast, dendritic distributions of Ncad and β-cat were unaffected by NMDA (Figure 9C). Loss of punctate colocalization of AKAP150 with Ncad and β-cat after NMDA treatment (Figure 9, A and B) was confirmed by measuring decreases in colocalization indices for AKAP150 with Ncad (#p < 0.05) and β-cat (#p < 0.01) (Figure 9C). Analysis of Ncad colocalization with Syp, a presynaptic marker, showed no change

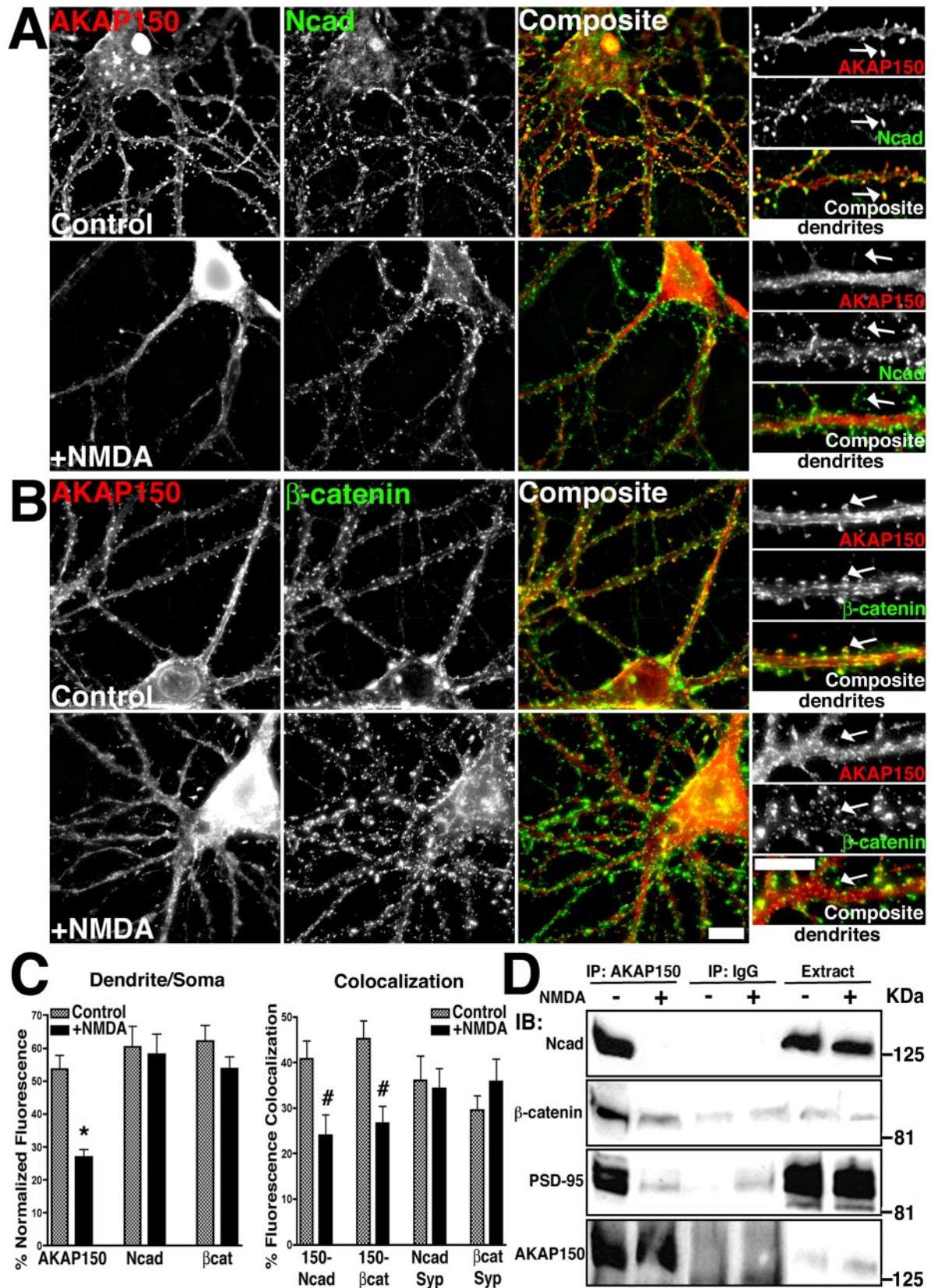


Figure 9. Regulation of AKAP79/150-cadherin complexes by NMDA receptor activation. (A and B) Loss of AKAP150 (red) dendritic spine colocalization (yellow) with Ncad (green) (A) and β -cat (green) (B) in response to NMDA (50 μ M, 37°C, 10 min) in hippocampal neurons. Smaller panels show magnification of dendrites, arrows point to colocalized signal in control spines and loss of spine colocalization after NMDA treatment. (C) Quantitation (n = 10 cells) showing a significant decrease in AKAP150, but not Ncad or β -cat, localization to dendrites

(Figure 9C), confirming maintenance of Ncad signal at synapses after NMDA treatment. Interestingly, β -cat showed a trend ($p = 0.33$) toward increased colocalization with Syp (Figure 9C), suggesting that the amount of β -cat in spines may be increased with NMDA, as seen in a previous study (Murase *et al.*, 2002). From these results, one would expect the complexes between AKAP79/150 and Ncad to dissociate with NMDA treatment. Accordingly, the ability to coprecipitate Ncad and β -cat with AKAP150 antibodies was lost after NMDA treatment (Figure 9D). Consistent with our published data (Gomez *et al.*, 2002), coprecipitation of PSD-95 family MAGUKs also was lost.

Because immunostaining visualizes cadherins expressed pre- and postsynaptically and AKAP79/150 is expressed only postsynaptically, we wanted to look selectively at the postsynaptic localization of Ncad upon NMDA treatment. In addition, we wanted to see whether the AKAP79 N-terminal domain involved in cadherin binding would on its own redistribute from dendrites in response to NMDA. To address these questions, hippocampal neurons were transfected with fluorescently tagged AKAP79, (1-153), Ncad, or PSD-95. Colocalization of AKAP79-YFP with endogenous AKAP150 and PSD-95 was seen on spines of transfected neurons (Figure 10A, arrows). In living neurons, AKAP79-YFP colocalized on spines with PSD-95-CFP in untreated neurons (Figure 10A, arrows) and even up to 5 min after the addition of NMDA (Figure 10B). However, from 10 to 40 min after NMDA addition, AKAP79-YFP showed progressive loss of concentrated fluorescence on spines and dendrite shaft plasma membranes with appearance of diffuse fluorescence in the cytoplasm of dendrite shafts and the soma (Figure 10B). At all time points, punctate clustering of PSD-95-CFP on spines was unaltered. Significant decreases in AKAP79-YFP colocalization with PSD-95-CFP ($^{\circ}p < 0.0001$), dendritic spine/shaft ratio ($*p < 0.001$), and dendrite/soma ratio ($\#p < 0.05$) were observed 30–40 min after NMDA (Figure 10F). Similar results were obtained when NMDA was applied for 3 min, washed out, and the neurons imaged 20–30 min later (our unpublished data).

AKAP79(1-153)-YFP also showed dendritic plasma membrane localization and substantial overlap with PSD-95-CFP on spines in control neurons (Figure 10C). In response to NMDA, (1-153)-YFP relocated from spines into the cytoplasm of dendrite shafts and the soma (Figure 10C, arrows). Significant decreases in PSD-95-CFP colocalization ($^{\circ}p < 0.001$), dendritic spine/shaft ratio ($*p < 0.0001$), and dendrite/soma ratio ($\#p < 0.05$) were measured after NMDA (Figure 10F). These results show that the N-terminal domain is sufficient to redistribute from postsynaptic membranes in response to NMDA. Under control conditions, Ncad-YFP colocalized with AKAP79-CFP (Figure 10E, arrows) or PSD-95-CFP (Figure 10D, arrows) on dendritic spines. In response to NMDA, Ncad-YFP did not significantly redistribute away from spines or from dendrites to the soma (Figure

10, D–F; no significant differences measured in PSD-95-CFP colocalization, spine/shaft, or dendrite/soma ratios). Thus, the model that emerges is that AKAP79/150 is lost, whereas cadherins, catenins, and PSD-95 remain localized to the postsynaptic membrane.

DISCUSSION

Postsynaptic targeting of AKAP79/150 depends on three MARCKS-like N-terminal basic domains that bind F-actin and acidic lipids (Dell'Acqua *et al.*, 1998; Gomez *et al.*, 2002). We now show that these domains also bind cadherins and direct AKAP79/150 to epithelial adherens junctions. Interestingly, our experiments show that PKC phosphorylation, Ca^{2+} -CaM binding, or high salt inhibit AKAP-cadherin binding in a manner similar to regulation of AKAP-F-actin and PIP_2 binding. These findings suggest that the three N-terminal basic clusters interact through electrostatics with multiple acidic membrane targets, and signaling events could coordinately regulate these interactions. Accordingly, NMDAR stimulation causes loss of AKAP79/150 postsynaptic membrane localization and loss of AKAP association with Ncad. Although the mechanism of this AKAP79/150 translocation is not fully understood, our studies to date indicate roles for Ca^{2+} influx, CaN activation, and F-actin depolymerization (Gomez *et al.*, 2002). These pathways are linked to AMPAR endocytosis and spine structural remodeling during LTD synaptic plasticity. Importantly, our previous work and work of others has implicated the AKAP, PKA, and CaN in regulation of AMPAR internalization and trafficking underlying plasticity (Beattie *et al.*, 2000; Esteban *et al.*, 2003). In addition, cadherins and CaN have been implicated in regulating spine structure and F-actin dynamics in synaptic plasticity (Okamura *et al.*, 2004; Zhou *et al.*, 2004). Thus, targeting of the AKAP signaling complexes to postsynaptic cadherins could help coordinate changes in synaptic structure and activity.

Electron microscopy studies have shown that AKAP79 and cadherins are enriched perisynaptically adjacent to the PSD (Uchida *et al.*, 1996; Sik *et al.*, 2000). Perisynaptic enrichment of cadherins is due to localization in an adhesion ring surrounding the PSD. Thus, binding to cadherins might help target AKAP79/150 to perisynaptic adhesions. A novel feature of this organization is that AKAP molecules could link MAGUK-AMPA complexes to cadherins, with the actin cytoskeleton serving as the master scaffold (Figure 11A). Additional cytoskeletal linkage of cadherins through catenins and AMPAR-SAP97 complexes through 4.1N and CASK would increase the importance of F-actin in this role (Lue *et al.*, 1996; Shen *et al.*, 2000; Karnak *et al.*, 2002; Rumbaugh *et al.*, 2003). Although our past results show that F-actin linkage is necessary for maintaining the AKAP and AMPAR at synapses, our current findings show that localization of AKAP79 in epithelial cells is regulated by cadherin signaling that maintains adherens junctions and cortical actin. In our experiments, low calcium-mediated disruption of cadherin adhesion resulted in a loss of AKAP from cell junctions, coincident with loss of cadherins from lateral membranes and actin reorganization. Thus, AKAP79/150 localization to dendritic spines also may be regulated by cadherins, both directly through protein-protein interactions and indirectly through cadherin signaling to spine actin.

Detection of FRET between AKAP79 and PKA or CaN at epithelial junctions supports a model where AKAP79/150 also might recruit PKA and CaN to perisynaptic adhesions in neurons (Figure 11). In particular, positioning MAGUK-

Figure 9 (cont). relative to the soma (dendrite/soma ratio, left-hand graph) and a significant loss of AKAP150 punctate colocalization with Ncad and β -cat (colocalization, left-hand graph) with NMDA. Colocalization of Ncad and β -cat with the presynaptic marker Syp was unchanged by NMDA ($n = 7$ cells). (D) Disruption of AKAP79/150 association with cadherins, catenins, and PSD-95 MAGUKs in response to NMDA. Approximately 7 mg of Triton-soluble extracts from control untreated (–) and NMDA treated (+) neurons were immunoprecipitated (IP:) with either 5 μ g of anti-AKAP150 or nonimmune IgG as indicated. IPs and cell extracts were probed (IB:) as indicated. Bars, 10 μ m.

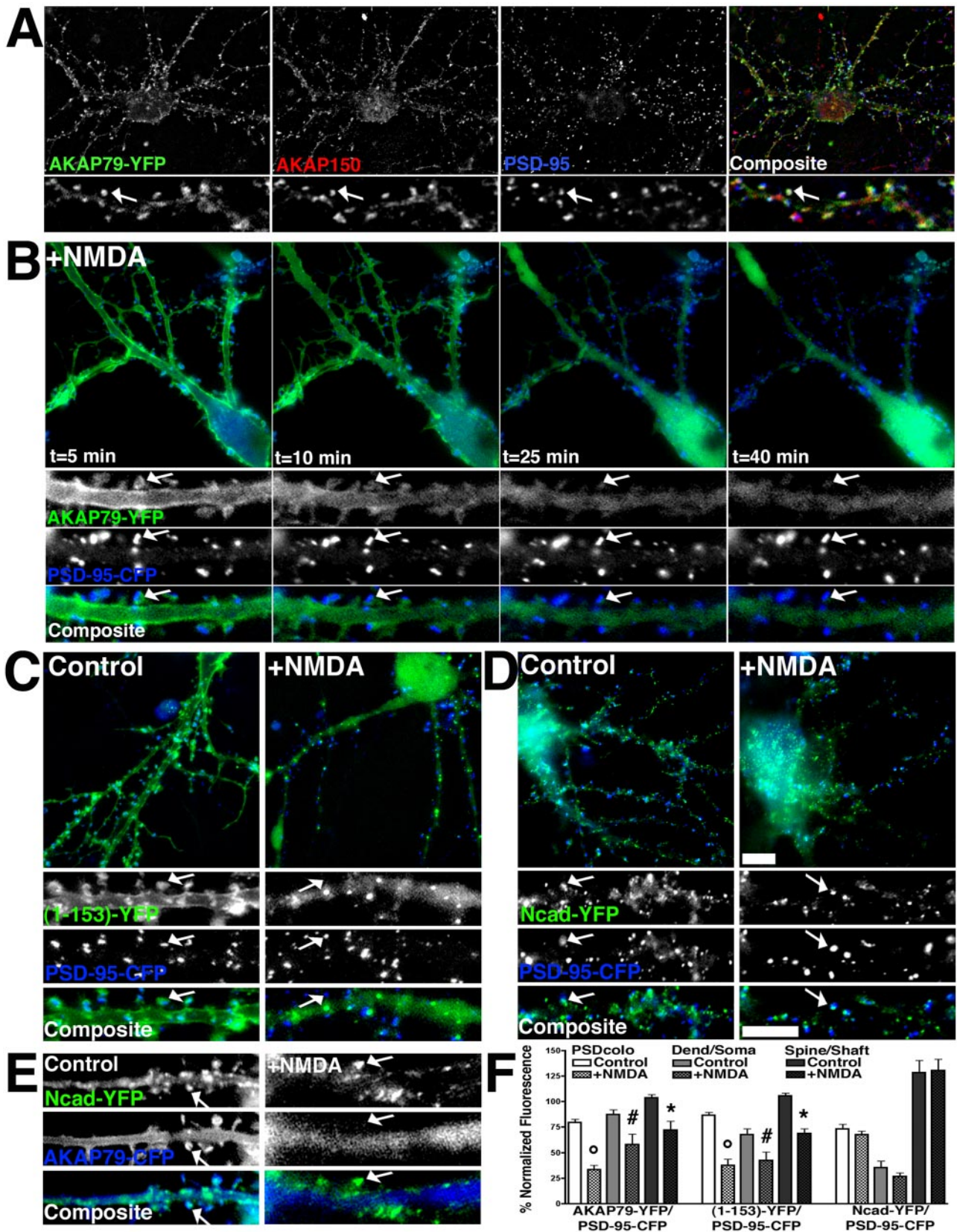


Figure 10. NMDA receptor regulation of AKAP79 postsynaptic localization with PSD-95 and Ncad imaged in living neurons. (A) AKAP79-YFP (green) colocalizes (arrow, white) on dendritic spines with endogenous rat AKAP150 (red) and PSD-95 (blue) in hippocampal neurons. (B) Time-lapse imaging in living hippocampal neurons of AKAP79-YFP (green) redistribution (arrows) away from PSD-95-CFP (blue) on dendritic spines in response to NMDA (50 μ M, 33°C, 5–40 min). (C) Postsynaptic localization of AKAP79(1-153)-YFP (green) with

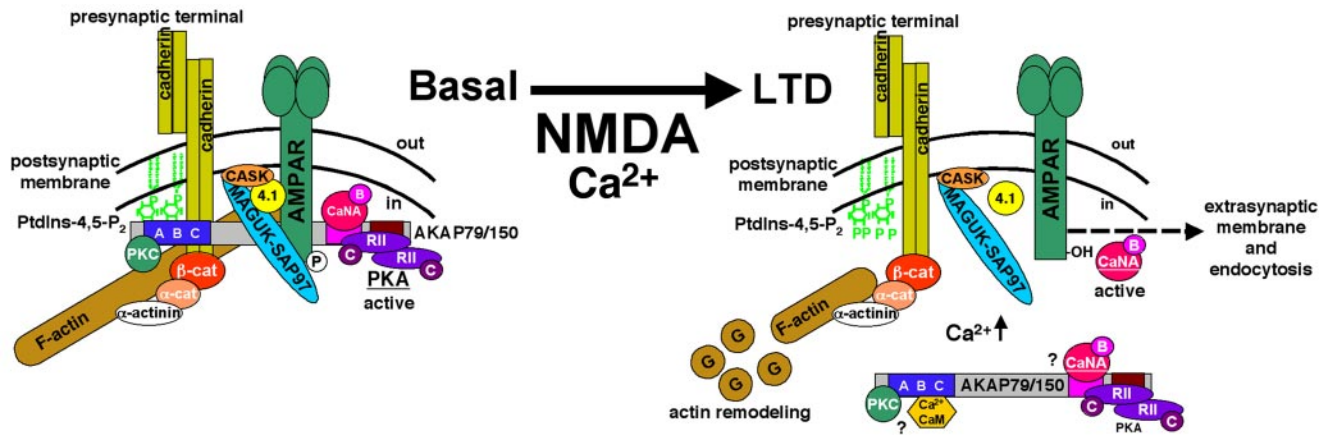


Figure 11. Model for NMDAR regulation of MAGUK–AKAP–cadherin signaling complexes at neuronal synapses. Under basal conditions, scaffold and anchoring proteins tether NMDAR and AMPAR to the actin cytoskeleton at the PSD. On NMDA stimulation and under LTD conditions, AKAP moves away from the PSD. Actin depolymerization and PKC or Ca^{2+} –CaM interactions with the targeting domain might participate in the disruption of AKAP targeting. AKAP takes with it PKA, leaving some CaN behind (Gomez *et al.*, 2002). This AKAP-mediated delocalization of PKA shifts the balance of AMPAR phosphorylation in favor of dephosphorylation. After dephosphorylation by CaN and PP1, AMPARs diffuse laterally out of the PSD, where they undergo CaN-dependent internalization and endocytosis. Actin depolymerization also is regulated by CaN and may participate in AMPAR untethering (Halpain *et al.*, 1998; Shen *et al.*, 2000). In contrast, cadherin–catenin complexes do not seem to be displaced in response to NMDA stimulation associated with LTD, despite reduction in spine F-actin (Okamoto *et al.*, 2004; Zhou *et al.*, 2004).

AKAP79–PKA/CaN complexes around the PSD, linked to cadherins, would provide an optimal geometry for regulating AMPAR phosphorylation. Under basal conditions, AKAP anchored PKA is active and CaN is inactive (Dell’Acqua *et al.*, 2002; Tavalin *et al.*, 2002). Thus, AKAP–cadherin complexes may define the borders of an area of high PKA and low CaN activity, with PKA acting as a sentry that maintains phosphorylation of AMPARs. In addition, large MAGUK–AKAP–cadherin–catenin complexes linked to actin also may be part of a physical barrier tethering linked AMPARs in synapses. In LTD, disrupting AKAP interactions with F-actin, MAGUKs and cadherins may remove part of the physical barrier retaining AMPARs in the PSD and also remove the anchored PKA that would keep AMPARs phosphorylated. Indeed, our previous work found that AKAP79/150 is likely to take PKA, but not much CaN, with it when leaving spines in response to NMDA treatments that also remove AMPAR from synapses (Gomez *et al.*, 2002). Importantly, LTP requires PKA phosphorylation of AMPAR–GluR1–Ser845 to promote synaptic stabilization of AMPARs, whereas LTD promotes dephosphorylation of this site by CaN and PP1 (Lee *et al.*, 2000; Esteban *et al.*, 2003; Lee *et al.*, 2003) and CaN-dependent AMPAR endocytosis

(Beattie *et al.*, 2000). In addition, NMDAR activation of CaN, acting against PKA, can lead to partial proteasome-mediated degradation of PSD-95 that may further reduce AMPAR synaptic tethering in LTD (Colledge *et al.*, 2003). In short, decreasing synaptic AKAP–PKA localization should favor removal of dephosphorylated AMPARs from synapses through multiple mechanisms (Figure 11).

A key question is whether AKAP79/150 regulates cadherins in these pathways to also control synaptic adhesion and structure. Cadherin adhesion is known to be important in plasticity; however, mechanisms for neuronal modulation of cadherins are poorly understood. Interestingly, our studies show that applications of NMDA that mimic LTD (Lee *et al.*, 1998; Beattie *et al.*, 2000) disrupt AKAP79/150 postsynaptic localization and association with cadherins without change in synaptic localization of Ncad or β -cat. Consistent with our studies, previous work has shown that NMDA treatments increased lateral *cis*-dimerization of cadherins (Tanaka *et al.*, 2000) and recruited β -cat into spines (Murase *et al.*, 2002), which should strengthen adhesion and actin linkage, thereby promoting cell contact retention. However, NMDA as well as low-frequency LTD electrical stimulation cause loss of spine F-actin, leading to thin filopodial spines that should favor decreased adhesion (Halpain *et al.*, 1998; Zhou *et al.*, 2004). Accordingly, overexpression of mutant Ncad that prevents adhesion produces filopodial spines (Togashi *et al.*, 2002). Thus, paradoxically LTD stimuli may favor cadherin– β -cat interaction despite changes in spine actin more consistent with decreased adhesion that favors loss of AKAP79/150. Cadherin regulation in LTP is also complex. During late phase LTP that is PKA dependent, Ncad is synthesized and recruited to synapses, suggesting increased adhesion with potentiation (Bozdagi *et al.*, 2000). In contrast, during early phase LTP, high-frequency stimulation may deplete extracellular Ca^{2+} and transiently disrupt cadherin adhesion through outside-in modulation (Tang *et al.*, 1998). However, this cadherin dispersion may be necessary for subsequent actin polymerization and spine enlargement accompanying LTP (Matsuzaki *et al.*, 2004;

Figure 10 (cont). PSD-95-CFP (blue) on dendritic spines (arrows) seen in control conditions is lost in response to NMDA. (D) Postsynaptic localization of Ncad-YFP (green) with PSD-95-CFP on dendritic spines (arrows) is unchanged in response to NMDA. (E) AKAP79-CFP (blue) redistributes away from Ncad-YFP (green) on dendritic spines in response to NMDA (arrows). (C–E) Post-NMDA 30–40 min; smaller panels in A–E show magnifications of dendrites, arrows mark spines where CFP/YFP colocalization is seen in control neurons but is not seen after NMDA treatment. (F) Quantitation ($n = 10$ cells) showing significant decreases in NMDA-treated relative to untreated controls for AKAP79-YFP and (1-153)-YFP but not Ncad-YFP localization to dendrites relative to the soma (dend/soma ratio), dendritic spines relative to the cytoplasm of dendrites shafts (spine/shaft ratio) and colocalization with PSD-95-CFP (PS-Dcolo). Bars, 10 μm .

Okamoto *et al.*, 2004; Okamura *et al.*, 2004). Thus, in both LTP and LTD, cadherin adhesion complexes may be reorganized over time through a combination of inside-out and outside-in mechanisms.

Inside-out regulation of cadherin adhesion can be achieved by several mechanisms. First, altering surface expression of cadherins through endocytosis can control adhesion in epithelial cells (Bryant and Stow, 2004). Interestingly, our findings suggest that AKAP79/150 may traffic with cadherins from the cell surface in response to extracellular Ca^{2+} depletion. Whether the AKAP, PKA and CaN regulate cadherin trafficking in this process is an interesting question as PKA and CaN have been implicated in AMPAR trafficking in neurons. Second, casein kinase II phosphorylation of cadherin increases affinity for β -cat (Huber and Weis, 2001), protecting against cadherin degradation (Huber *et al.*, 2001) and ultimately strengthening adhesion. However, neither PKA nor CaN have been directly implicated in the regulation of cadherin phosphorylation. Finally, controlling expression levels of cadherin binding partners can regulate adhesion. For example, neuronal overexpression of α -cat leads to more numerous and stable dendritic spines, whereas genetic deletion of neuronal α -cat leads to spine loss (Abe *et al.*, 2004). Overexpression of β -cat also can increase spine numbers, depending on developmental stage (Yu and Malenka, 2004).

In AKAP79/150, we mapped the AKAP binding site to a conserved acidic region within the cadherin β -cat binding site, suggesting possible competition in AKAP and β -cat binding; however, no competition was seen using *in vitro* binding assays. In addition, consistent with AKAP–cadherin–catenin ternary complex formation *in vivo*, AKAP79/150 colocalizes with cadherins and β -cat on spines and lateral membranes, and all three proteins coprecipitate from cell and tissue extracts. Furthermore, overexpression of AKAP79 in MDCK cells leads to colocalization with β -cat and Ecad at lateral adhesions as opposed to β -cat displacement. This is in contrast to the displacement of β -cat and inhibition of adhesion seen in cells overexpressing $G\alpha_{12}$, which also binds to Ecad in the β -cat binding domain, although in a more C-terminal region than AKAP (Kaplan *et al.*, 2001; Meigs *et al.*, 2001, 2002). Thus, it is possible that AKAP binding blocks only a small subregion of the large β -cat binding surface in Ecad, allowing sufficient remaining contacts to preserve β -cat binding and adhesion. Another possibility is that because cadherins form *cis*-dimers, AKAP79/150 might bind to one monomer, whereas β -cat binds the other. Finally, AKAP binding to cadherin–catenin complexes may be stabilized by additional proteins *in vivo*. For example, AKAP79/150 has been reported to interact with IQGAP, a Rac/Cdc42 regulatory protein that binds cadherins and catenins to regulate signaling to actin (Briggs and Sacks, 2003; Nauert *et al.*, 2003). Thus, AKAP79/150 could play a complex role in cadherin regulation both through direct interaction and through regulation of anchored signaling proteins. Elucidating novel functions of AKAP79/150 targeting to cadherins in both neurons and epithelial cells will be an exciting challenge.

ACKNOWLEDGMENTS

We thank Shuvo Alam, Emily Gibson (University of Colorado at Denver and Health Sciences Center, Denver, CO), and Adam Bishop (Howard Hughes Medical Institute, Oregon Health Sciences University, Portland, OR) for technical assistance. We thank Eric Horne, Dr. Naoto Hoshi, Dr. Deanna Benson, Dr. Patrick Casey, Dr. William Weis, Dr. Al El-Husseini, Dr. Ben Margolis (University of Michigan, Ann Arbor, MI), Dr. Yvonne Lai, and Dr. Rytis Prekeris (University of Colorado at Denver and Health Sciences Center) for

reagents used in this study. This work was supported by Grants AHA0420034Z (to J.A.G.), GM-48231 (to J.D.S.), and NS-40701 (to M.L.D.).

REFERENCES

- Abe, K., Chisaka, O., Van Roy, F., and Takeichi, M. (2004). Stability of dendritic spines and synaptic contacts is controlled by α -N-catenin. *Nat. Neurosci.* 7, 357–363.
- Banke, T. G., Bowie, D., Lee, H., Haganir, R. L., Schousboe, A., and Traynelis, S. F. (2000). Control of GluR1 AMPA receptor function by cAMP-dependent protein kinase. *J. Neurosci.* 20, 89–102.
- Bauman, A. L., Goehring, A. S., and Scott, J. D. (2004). Orchestration of synaptic plasticity through AKAP signaling complexes. *Neuropharmacology* 46, 299–310.
- Beattie, E. C., Carroll, R. C., Yu, X., Morishita, W., Yasuda, H., von Zastrow, M., and Malenka, R. C. (2000). Regulation of AMPA receptor endocytosis by a signaling mechanism shared with LTD. *Nat. Neurosci.* 3, 1291–1300.
- Bozdagi, O., Shan, W., Tanaka, H., Benson, D. L., and Huntley, G. W. (2000). Increasing numbers of synaptic puncta during late-phase LTP: N-cadherin is synthesized, recruited to synaptic sites, and required for potentiation. *Neuron* 28, 245–259.
- Bredt, D. S. (1998). Sorting out genes that regulate epithelial and neuronal polarity. *Cell* 94, 691–694.
- Briggs, M. W., and Sacks, D. B. (2003). IQGAP proteins are integral components of cytoskeletal regulation. *EMBO Rep.* 4, 571–574.
- Bryant, D. M., and Stow, J. L. (2004). The ins and outs of E-cadherin trafficking. *Trends Cell Biol.* 14, 427–434.
- Carroll, R. C., Beattie, E. C., von Zastrow, M., and Malenka, R. C. (2001). Role of AMPA receptor endocytosis in synaptic plasticity. *Nat. Rev. Neurosci.* 2, 315–324.
- Colledge, M., Dean, R. A., Scott, G. K., Langeberg, L. K., Haganir, R. L., and Scott, J. D. (2000). Targeting of PKA to glutamate receptors through a MAGUK-AKAP complex. *Neuron* 27, 107–119.
- Colledge, M., Snyder, E. M., Crozier, R. A., Soderling, J. A., Jin, Y., Langeberg, L. K., Lu, H., Bear, M. F., and Scott, J. D. (2003). Ubiquitination regulates PSD-95 degradation and AMPA receptor surface expression. *Neuron* 40, 595–607.
- Dell'Acqua, M. L., Dodge, K. L., Tavalin, S. J., and Scott, J. D. (2002). Mapping the protein phosphatase-2B anchoring site on AKAP79. Binding and inhibition of phosphatase activity are mediated by residues 315–360. *J. Biol. Chem.* 277, 48796–48802.
- Dell'Acqua, M. L., Faux, M. C., Thorburn, J., Thorburn, A., and Scott, J. D. (1998). Membrane-targeting sequences on AKAP79 bind phosphatidylinositol-4,5-bisphosphate. *EMBO J.* 17, 2246–2260.
- Esteban, J. A., Shi, S. H., Wilson, C., Nuriya, M., Haganir, R. L., and Malinow, R. (2003). PKA phosphorylation of AMPA receptor subunits controls synaptic trafficking underlying plasticity. *Nat. Neurosci.* 6, 136–143.
- Gomez, L. L., Alam, S., Smith, K. E., Horne, E., and Dell'Acqua, M. L. (2002). Regulation of A-kinase anchoring protein 79/150-cAMP-dependent protein kinase postsynaptic targeting by NMDA receptor activation of calcineurin and remodeling of dendritic actin. *J. Neurosci.* 22, 7027–7044.
- Halpain, S., Hipolito, A., and Saffer, L. (1998). Regulation of F-actin stability in dendritic spines by glutamate receptors and calcineurin. *J. Neurosci.* 18, 9835–9844.
- Huber, A. H., Stewart, D. B., Laurents, D. V., Nelson, W. J., and Weis, W. I. (2001). The cadherin cytoplasmic domain is unstructured in the absence of beta-catenin. A possible mechanism for regulating cadherin turnover. *J. Biol. Chem.* 276, 12301–12309.
- Huber, A. H., and Weis, W. I. (2001). The structure of the beta-catenin/E-cadherin complex and the molecular basis of diverse ligand recognition by beta-catenin. *Cell* 105, 391–402.
- Kaplan, D. D., Meigs, T. E., and Casey, P. J. (2001). Distinct regions of the cadherin cytoplasmic domain are essential for functional interaction with $G\alpha_{12}$ and β -catenin. *J. Biol. Chem.* 276, 44037–44043.
- Karnak, D., Lee, S., and Margolis, B. (2002). Identification of multiple binding partners for the amino-terminal domain of synapse-associated protein 97. *J. Biol. Chem.* 277, 46730–46735.
- Kartenbeck, J., Schmelz, M., Franke, W. W., and Geiger, B. (1991). Endocytosis of junctional cadherins in bovine kidney epithelial (MDBK) cells cultured in low Ca^{2+} ion medium. *J. Cell Biol.* 113, 881–892.

- Lee, H. K., Barbarosie, M., Kameyama, K., Bear, M. F., and Huganir, R. L. (2000). Regulation of distinct AMPA receptor phosphorylation sites during bidirectional synaptic plasticity. *Nature* 405, 955–959.
- Lee, H. K., Kameyama, K., Huganir, R. L., and Bear, M. F. (1998). NMDA induces long-term synaptic depression and dephosphorylation of the GluR1 subunit of AMPA receptors in hippocampus. *Neuron* 21, 1151–1162.
- Lee, H. K., *et al.* (2003). Phosphorylation of the AMPA receptor GluR1 subunit is required for synaptic plasticity and retention of spatial memory. *Cell* 112, 631–643.
- Lue, R. A., Brandin, E., Chan, E. P., and Branton, D. (1996). Two independent domains of hDlg are sufficient for subcellular targeting: the PDZ1–2 conformational unit and an alternatively spliced domain. *J. Cell Biol.* 135, 1125–1137.
- Malenka, R. C., and Bear, M. F. (2004). LTP and LTD: an embarrassment of riches. *Neuron* 44, 5–21.
- Matsuzaki, M., Honkura, N., Ellis-Davies, G. C., and Kasai, H. (2004). Structural basis of long-term potentiation in single dendritic spines. *Nature* 429, 761–766.
- McLaughlin, S., and Aderem, A. (1995). The myristoyl-electrostatic switch: a modulator of reversible protein-membrane interactions. *Trends Biochem. Sci.* 20, 272–276.
- Meigs, T. E., Fedor-Chaiken, M., Kaplan, D. D., Brackenbury, R., and Casey, P. J. (2002). Galpha12 and Galpha13 negatively regulate the adhesive functions of cadherin. *J. Biol. Chem.* 277, 24594–24600.
- Meigs, T. E., Fields, T. A., McKee, D. D., and Casey, P. J. (2001). Interaction of α 12 and α 13 with the cytoplasmic domain of cadherin provides a mechanism for beta-catenin release. *Proc. Natl. Acad. Sci. USA* 98, 519–524.
- Murase, S., Mosser, E., and Schuman, E. M. (2002). Depolarization drives beta-Catenin into neuronal spines promoting changes in synaptic structure and function. *Neuron* 35, 91–105.
- Nauert, J. B., Rigas, J. D., and Lester, L. B. (2003). Identification of an IQGAP1/AKAP79 complex in beta-cells. *J. Cell Biochem.* 90, 97–108.
- Okamoto, K., Nagai, T., Miyawaki, A., and Hayashi, Y. (2004). Rapid and persistent modulation of actin dynamics regulates postsynaptic reorganization underlying bidirectional plasticity. *Nat. Neurosci.* 7, 1104–1112.
- Okamura, K., Tanaka, H., Yagita, Y., Saeki, Y., Taguchi, A., Hiraoka, Y., Zeng, L. H., Colman, D. R., and Miki, N. (2004). Cadherin activity is required for activity-induced spine remodeling. *J. Cell Biol.* 167, 961–972.
- Oliveria, S. F., Gomez, L. L., and Dell'Acqua, M. L. (2003). Imaging kinase-AKAP79-phosphatase scaffold complexes at the plasma membrane in living cells using FRET microscopy. *J. Cell Biol.* 160, 101–112.
- Pokutta, S., and Weis, W. I. (2002). The cytoplasmic face of cell contact sites. *Curr. Opin. Struct. Biol.* 12, 255–262.
- Reuver, S. M., and Garner, C. C. (1998). E-cadherin mediated cell adhesion recruits SAP97 into the cortical cytoskeleton. *J. Cell Sci.* 111, 1071–1080.
- Roura, S., Miravet, S., Piedra, J., Garcia de Herreros, A., and Dunach, M. (1999). Regulation of E-cadherin/Catenin association by tyrosine phosphorylation. *J. Biol. Chem.* 274, 36734–36740.
- Rumbaugh, G., Sia, G. M., Garner, C. C., and Huganir, R. L. (2003). Synapse-associated protein-97 isoform-specific regulation of surface AMPA receptors and synaptic function in cultured neurons. *J. Neurosci.* 23, 4567–4576.
- Shen, L., Liang, F., Walensky, L. D., and Huganir, R. L. (2000). Regulation of AMPA receptor GluR1 subunit surface expression by a 4. 1N-linked actin cytoskeletal association. *J. Neurosci.* 20, 7932–7940.
- Sik, A., Gulacsi, A., Lai, Y., Doyle, W. K., Pacia, S., Mody, I., and Freund, T. F. (2000). Localization of the A kinase anchoring protein AKAP79 in the human hippocampus. *Eur. J. Neurosci.* 12, 1155–1164.
- Smith, F. D., and Scott, J. D. (2002). Signaling complexes: junctions on the intracellular information super highway. *Curr. Biol.* 12, R32–R40.
- Sugimoto, K., Honda, S., Yamamoto, T., Ueki, T., Monden, M., Kaji, A., Matsumoto, K., and Nakamura, T. (1996). Molecular cloning and characterization of a newly identified member of the cadherin family, PB-cadherin. *J. Biol. Chem.* 271, 11548–11556.
- Tanaka, H., Shan, W., Phillips, G. R., Arndt, K., Bozdagi, O., Shapiro, L., Huntley, G. W., Benson, D. L., and Colman, D. R. (2000). Molecular modification of N-cadherin in response to synaptic activity. *Neuron* 25, 93–107.
- Tang, L., Hung, C. P., and Schuman, E. M. (1998). A role for the cadherin family of cell adhesion molecules in hippocampal long-term potentiation. *Neuron* 20, 1165–1175.
- Tavalin, S. J., Colledge, M., Hell, J. W., Langeberg, L. K., Huganir, R. L., and Scott, J. D. (2002). Regulation of GluR1 by the A-kinase anchoring protein 79 (AKAP79) signaling complex shares properties with long-term depression. *J. Neurosci.* 22, 3044–3051.
- Togashi, H., Abe, K., Mizoguchi, A., Takaoka, K., Chisaka, O., and Takeichi, M. (2002). Cadherin regulates dendritic spine morphogenesis. *Neuron* 35, 77–89.
- Uchida, N., Honjo, Y., Johnson, K. R., Wheelock, M. J., and Takeichi, M. (1996). The catenin/cadherin adhesion system is localized in synaptic junctions bordering transmitter release zones. *J. Cell Biol.* 135, 767–779.
- Yap, A. S., and Kovacs, E. M. (2003). Direct cadherin-activated cell signaling: a view from the plasma membrane. *J. Cell Biol.* 160, 11–16.
- Yu, X., and Malenka, R. C. (2004). Multiple functions for the cadherin/catenin complex during neuronal development. *Neuropharmacology* 47, 779–786.
- Zhou, Q., Homma, K. J., and Poo, M. M. (2004). Shrinkage of dendritic spines associated with long-term depression of hippocampal synapses. *Neuron* 44, 749–757.